Marrying Lasers and Particle Beams

Luca Serafini – INFN Milan

- **Common Aspects of Laser and Particle Beams: Brilliance, Brightness, Phase space density, e.m. field intensity**
- **Interactions: to exchange informations (diagnostics), to exchange energy/momentum (laser based accelerators, vs. RF), to exchange order (coherence) or disorder (heating)**
- **3 Examples of interactions in vacuum:**
  Seeded FEL, Inverse FEL, Compton Sources
- **Future directions**

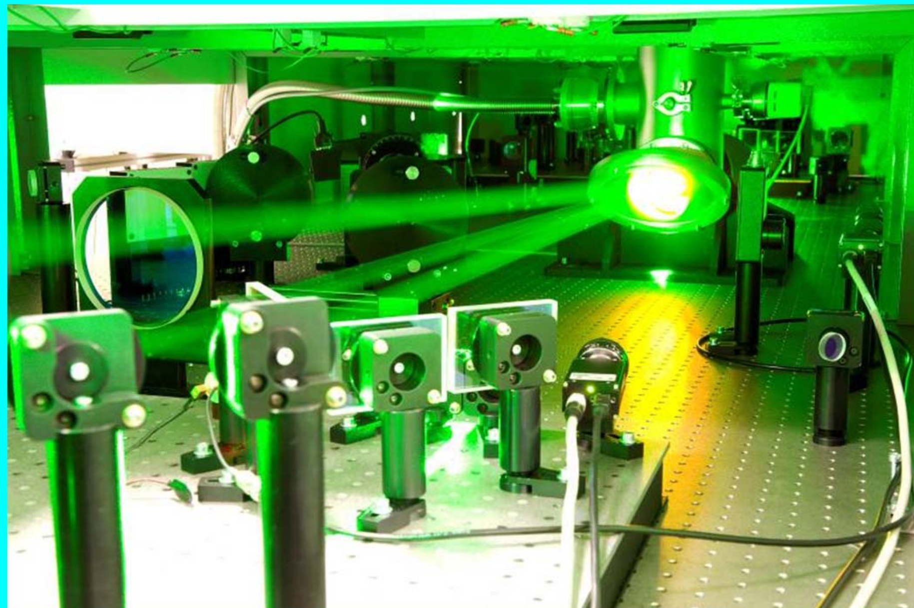

Lasers are Beams and propagate in free space, under the effect of diffraction, just like particle beams under the effect of their emittance

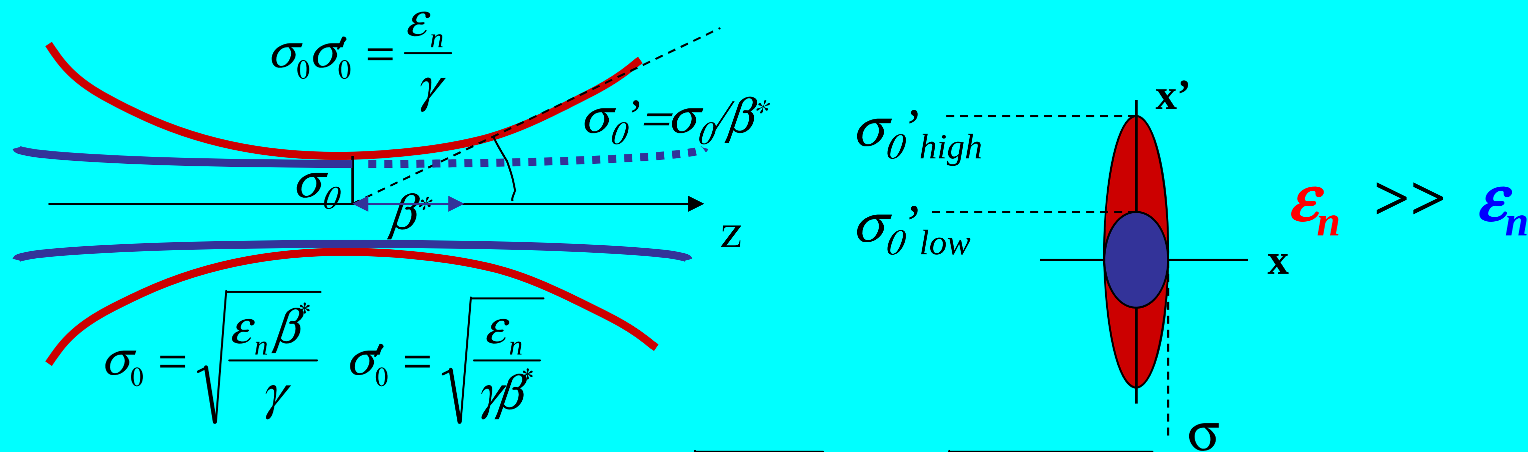

$$\sigma(z) = \sigma_0 \sqrt{1 + \frac{z^2}{\beta^{*2}}} = \sigma_0 \sqrt{1 + \frac{\varepsilon_n^2}{\gamma^2 \sigma_0^4} z^2}$$

TEM$_{00}$ Gaussian Laser mode (circular polarization M^2=1 diffraction limited)

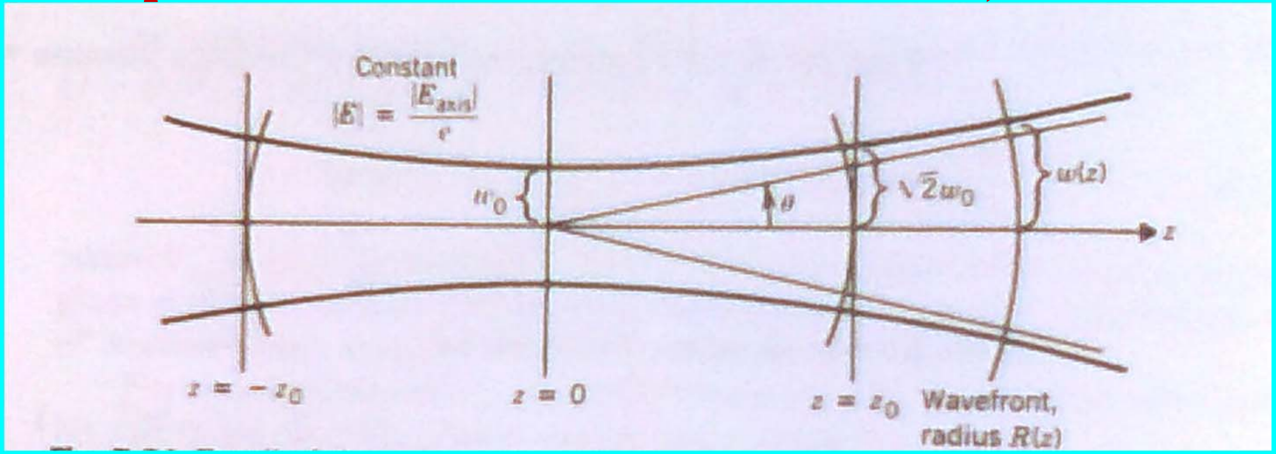

$$E_0(x,y,z,t) = A_0 e^{i\omega t} e^{-ikz} \frac{Z_0}{Z_0 - iz} \exp\left[-\frac{k\left(x^2+y^2\right)}{2} \frac{1}{Z_0 - iz} \right] \quad k = 2\pi/\lambda$$

$$\left|E_0(x,y,z,t)\right| = E_0 \frac{w_0}{w} e^{-\frac{x^2+y^2}{w^2}}$$

$$w = w_0\sqrt{1+\frac{z^2}{Z_0^2}} \qquad Z_0 = \frac{\pi w_0^2}{\lambda} \qquad \vartheta = \frac{w_0}{Z_0} = \frac{\lambda}{\pi w_0}$$

$$I \propto \left|E_0(x,y,z,t)\right|^2$$

LASER

$$Z_0 = \frac{4\pi\left(\frac{w_0}{2}\right)^2}{\lambda}$$

$$\frac{w}{2} = \frac{w_0}{2}\sqrt{1+\frac{z^2}{Z_0^2}}$$

PARTICLE BEAM

$$\beta^* = \frac{\sigma_0^2}{\varepsilon_n/\gamma}$$

$$\sigma(z) = \sigma_0\sqrt{1+\frac{z^2}{\beta^{*2}}}$$

$$\frac{\lambda}{4\pi} = \frac{\varepsilon_n}{\gamma} \quad and \quad w_0 = 2\sigma_0$$

$$\varepsilon_n \le \frac{\lambda_{FEL}\gamma}{4\pi}$$

$$w(z) = 2\sigma(z) \quad and \quad \vartheta(z) = 2\sigma'(z)$$

Marrying Lasers and Particle Beams

The Figure of Merits for Lasers and Beams

Brilliance of Lasers and X-ray sources

$$N_{ph} = 10^{19} - 10^{20}$$

$$\sigma_t = 10 - 20 \quad fs$$

ELI

BELLA

$$B = \frac{N_{ph}}{\sqrt{2\pi}\sigma_t \left(M^2 \lambda\right)^2 \frac{\Delta\lambda}{\lambda}}$$

$$a_0 = 4.3 \frac{\lambda}{w_0} \sqrt{\frac{U[J]}{\sigma_t[ps]}}$$

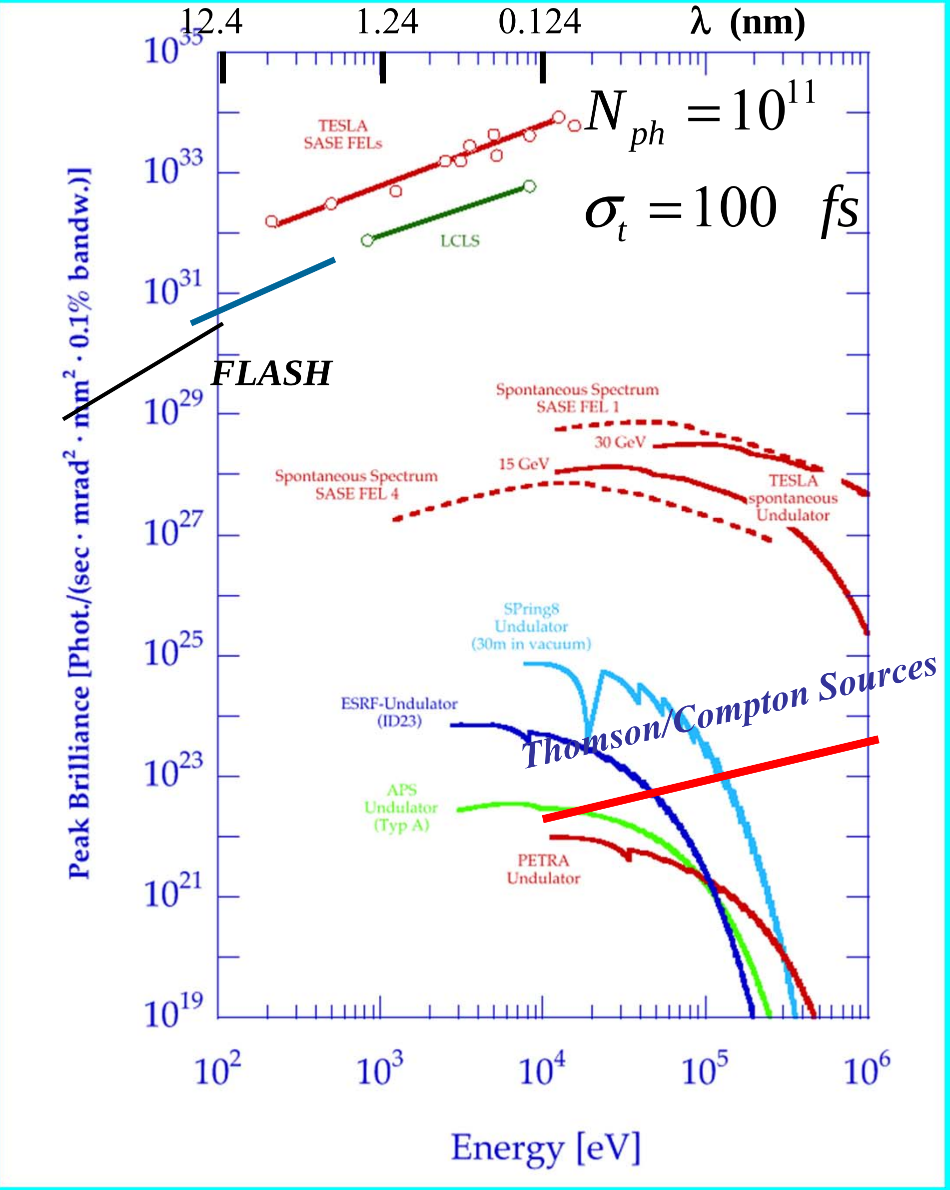

$$B_n = \frac{2I}{\varepsilon_n^2}$$

fsec bunches
laser-plasma

0.1-1 psec bunches
RF

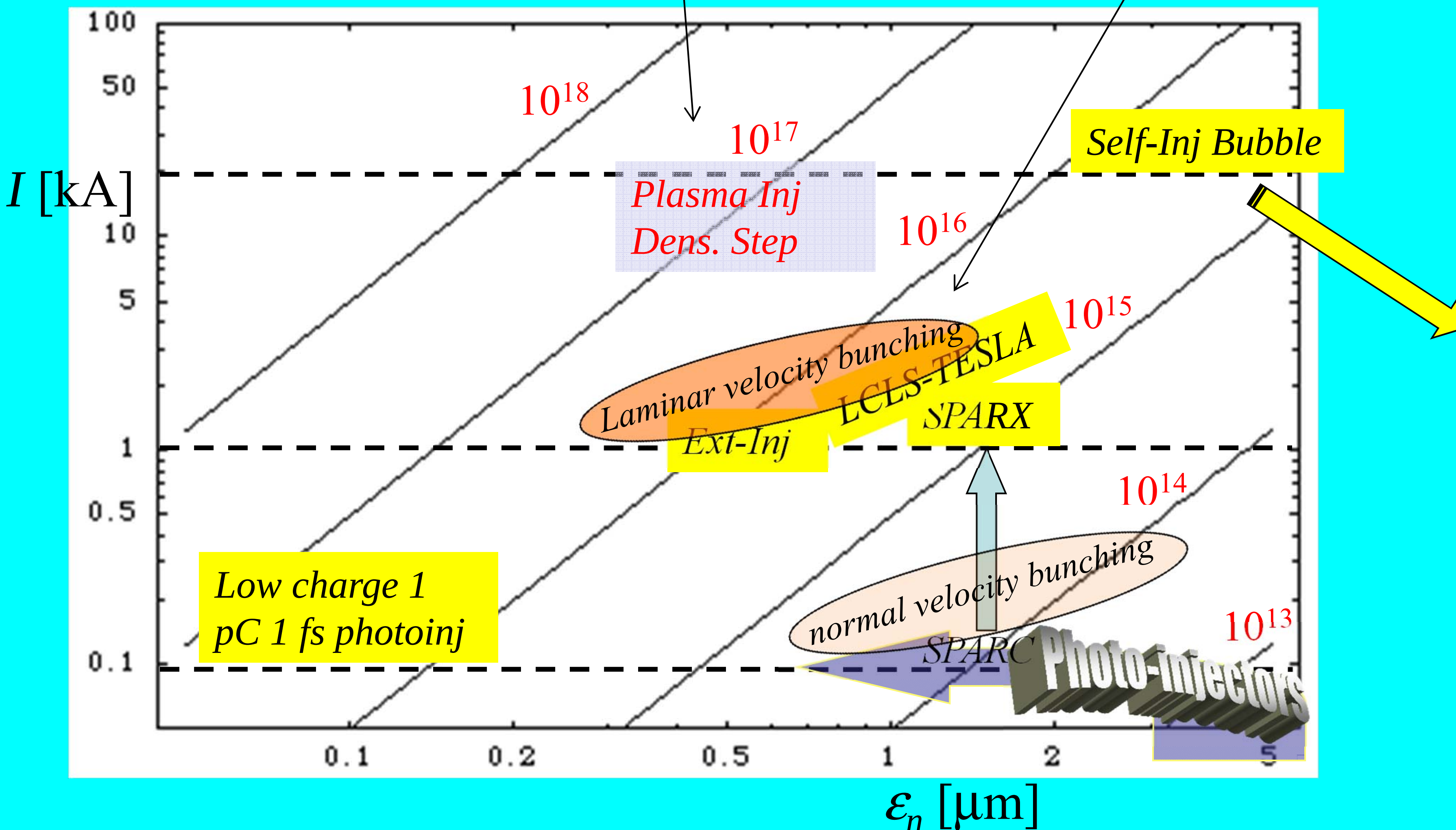

The Electron Beam Brightness Chart [A/(m·rad)^2]

$$B_{6D} = \frac{2I}{\frac{\Delta\gamma}{\gamma}\varepsilon_n^2} = \frac{B_n}{\frac{\Delta\gamma}{\gamma}}$$

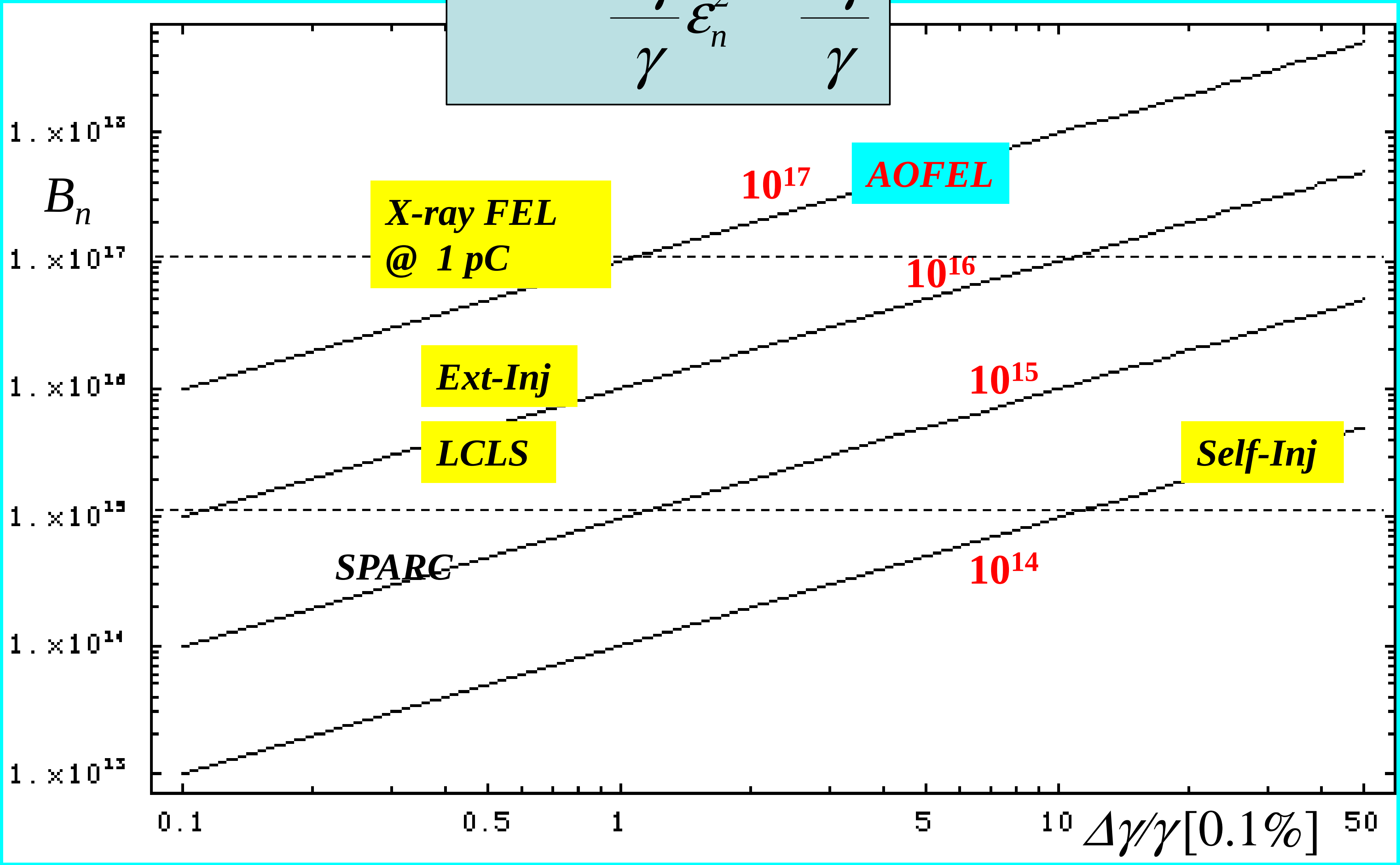

The 6D Brilliance Chart [A/((m·rad)^{2}0.1%)]

$$\mathcal{B}_{6D}=\frac{2I}{\frac{\Delta\gamma}{\gamma}\varepsilon_n^2}=\frac{B_n}{\frac{\Delta\gamma}{\gamma}}$$

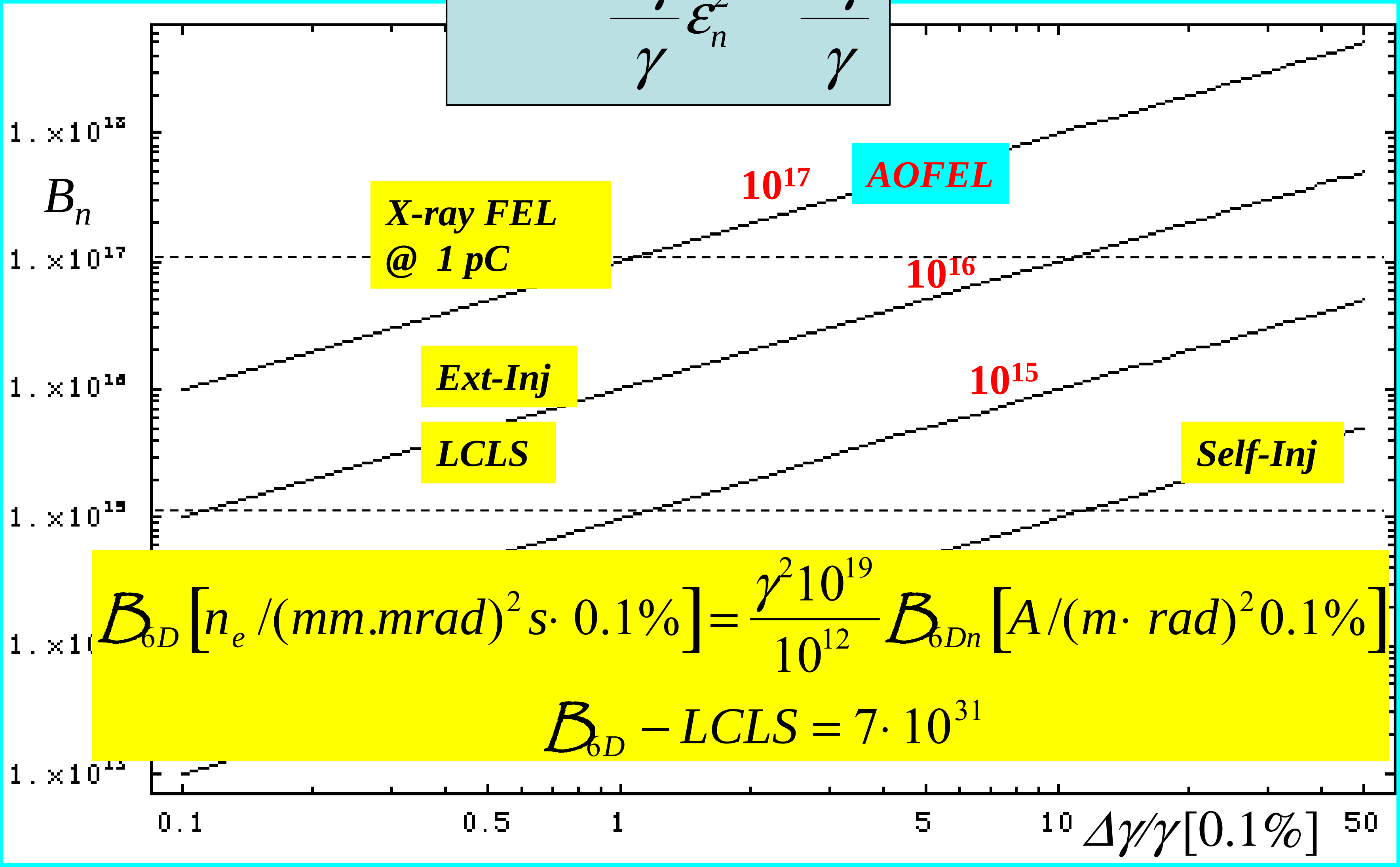

$$\mathcal{B}_{6D}\left[n_e/(mm.mrad)^2 s\cdot 0.1\%\right]=\frac{\gamma^2 10^{19}}{10^{12}}\mathcal{B}_{6Dn}\left[A/(m\cdot rad)^2 0.1\%\right]$$

$$\mathcal{B}_{6D}-LCLS=7\cdot 10^{31}$$

The 6D Brilliance Chart [A/((m·rad)^{2}0.1%)]

Electric field carried by laser $E_{\perp} \propto \sqrt{I}$

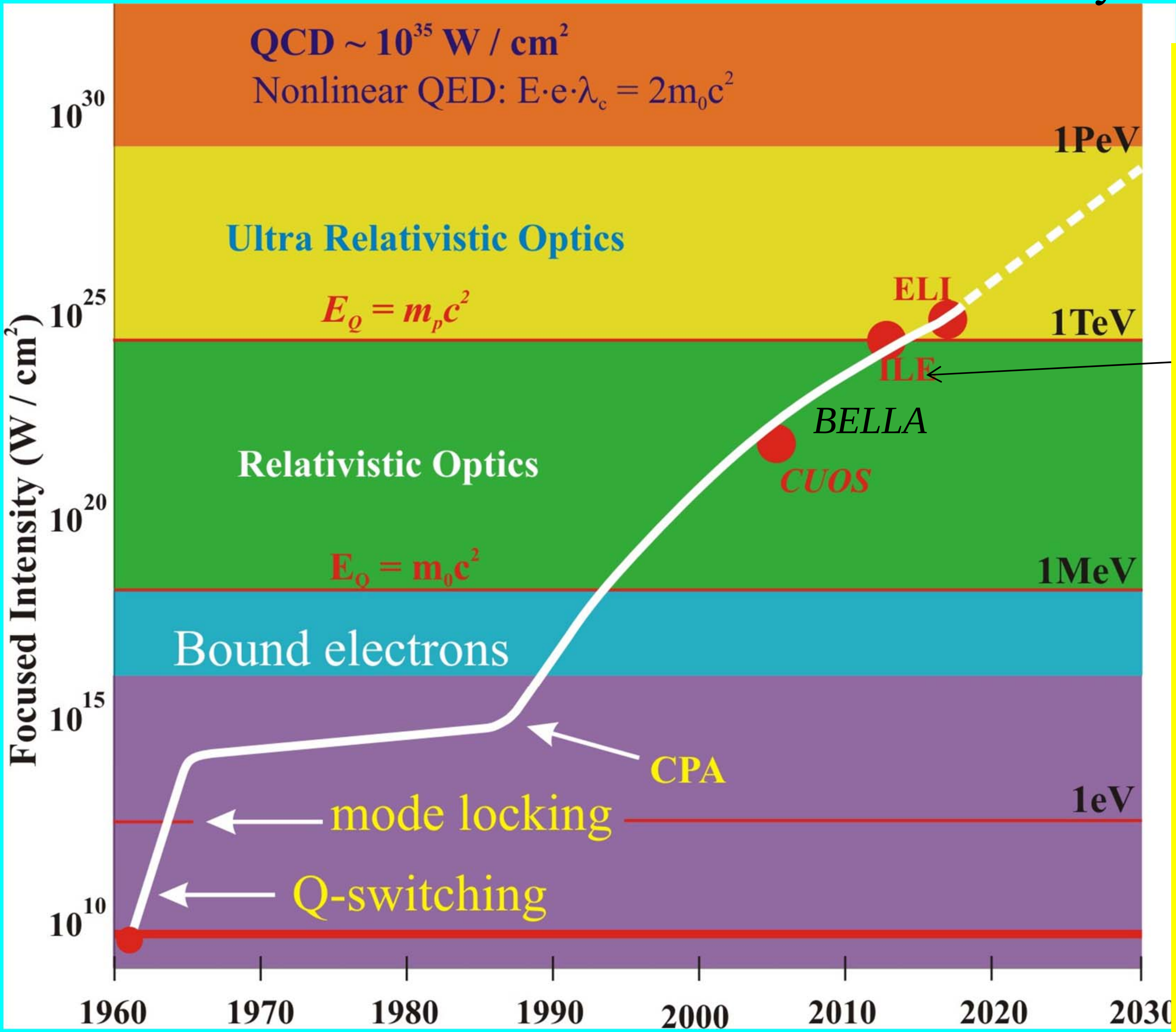

APOLLON laser for ELI

- 2·10 PW
- 15 fs
- ~ 1/min
- 10^{24} W/cm^2
- $a_0 = 35$
- 2.5x10^3 TV/m

(Schwinger's field 10^6 TV/m)

- **BELLA 1 PW**
- 5x10^{22} W/cm^2
- 1 Hz
- $a_0 = 10$
- 600 TV/m

Courtesy G. Mourou

e.m. field carried by the electron bunch

- With 2 fs LCLS beam we have $E_r^{edge} = \dfrac{\eta_0 I}{2\pi\sigma}$
- For 2-20 pC beam, we have *1 TV/m fields* (!)

PWFA Plasma Acceleration

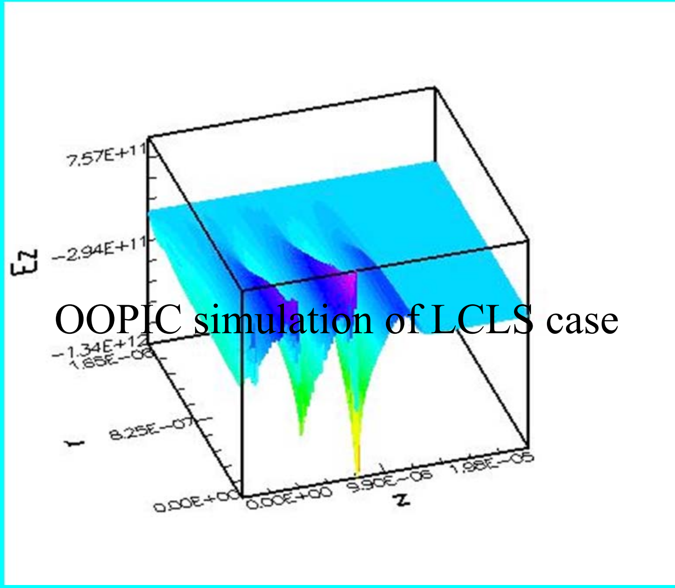

OOPIC simulation of LCLS case

1 TV/m accelerating field: a dream for a table-top TeV-class e^-e^+ collider?

e.m. field carried by the electron bunch

- With 2 fs LCLS beam we have $E_r^{edge} = \dfrac{\eta_0 I}{2\pi\sigma}$
- For 2-20 pC beam, we have *1 TV/m fields* (!)

PWFA Plasma Acceleration

case

Teravolt-per-meter plasma wakefields from low-charge, femtosecond electron beams

J. B. Rosenzweig*, G. Andonian*, P. Bucksbaum†, M. Ferrario[1], S. Full*,
A. Fukusawa*, E. Hemsing*, M. Hogan†, P. Krejcik†, P. Muggli[2], G. Marcus*,
A. Marinelli*, P. Musumeci*, B. O'Shea*, C. Pellegrini*, D. Schiller*, and G. Travish*
*Department of Physics and Astronomy, University of California Los Angeles, Los Angeles, California 90095, USA
†Stanford Linear Accelerator Center, Menlo Park, CA
[1] Istituto Nazionale di Fisica Nucleare Laboratori Nazionali di Frascati, via Enrico Fermi 40, Frascati (RM) Italy and
[2] University of Southern California, Dept. of Engineering Physics, Los Angeles, CA
(Dated: November 12, 2009)

Recent initiatives in ultra-short, GeV electron beam generation have focused on achieving sub-fs pulses for driving X-ray free-electron lasers (FELs) in single-spike mode. This scheme employs very low charge beams, which may allow existing FEL injectors to produce few-100 as pulses, with high brightness. Towards this end, recent experiments at SLAC have produced ~2 fs rms, low transverse emittance, 20 pC electron pulses. Here we examine use of such pulses to excite plasma wakefields exceeding 1 TV/m. We present a focusing scheme capable of producing <200 nm beam sizes, where the surface Coulomb fields are also ~TV/m. These conditions access a new regime for high field atomic physics, allowing frontier experiments, including sub-fs plasma formation for wake excitation.

PACS numbers: 41.60.Cr, 41.75.-i, 41.85.Gy, 42.60.Jf

PHYSICAL REVIEW SPECIAL TOPICS - ACCELERATORS AND BEAMS 11, 070703 (2008)

Ultrahigh brightness electron beams by plasma-based injectors for driving all-optical free-electron lasers

V. Petrillo,[1,2] L. Serafini,[1] and P. Tomassini[1,3]
[1]*INFN-Milan, Via Celoria 16, 20133, Milano, Italy*
[2]*Università degli Studi di Milano, Dipartimento di Fisica, Via Celoria 16, 20133, Milano, Italy*
[3]*CNR-ILIL, Via G. Moruzzi, 1, 56124, Pisa, Italy*
(Received 27 March 2008; published 29 July 2008)

SPARC_LAB

$$E_r^{edge} = \frac{\eta_0 I}{2\pi\sigma} \quad I = 20 \ kA; \ \sigma = 1 \ \mu m \quad E_r^{edge} = 1 \ TV/m$$

Longitudinal Phase Space distributions show violent blow-up of uncorrelated energy spread due to transverse space charge field (electrons are fermions…)

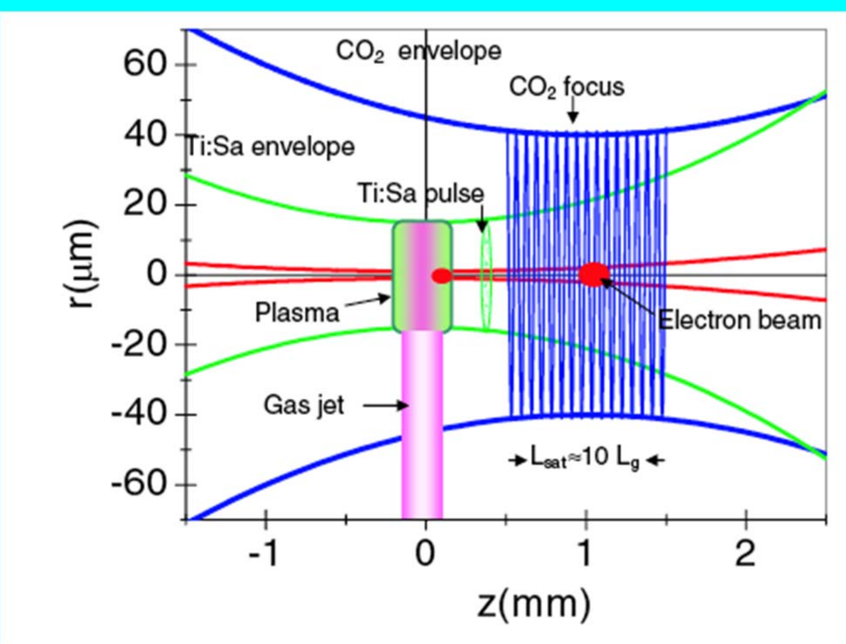

158 µm from plasma exit, about 3 gain lenghts

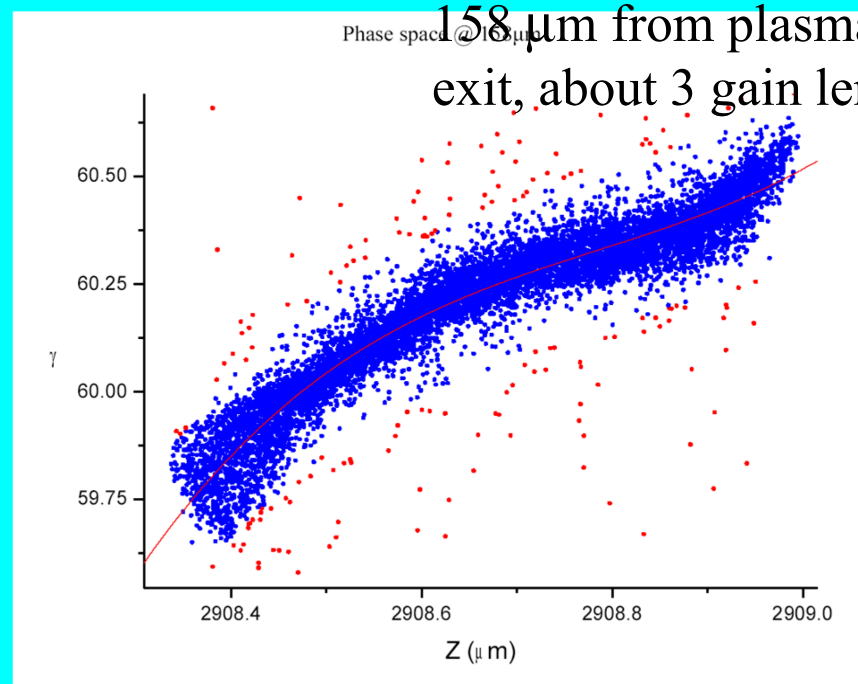

Marrying Lasers and Particle Beams

Seeding a High Gain Free Electron Laser: transfer coherence from the Laser to the FEL radiation through the Electron Beam

Seeding @ SPARC

ENEA

INFN

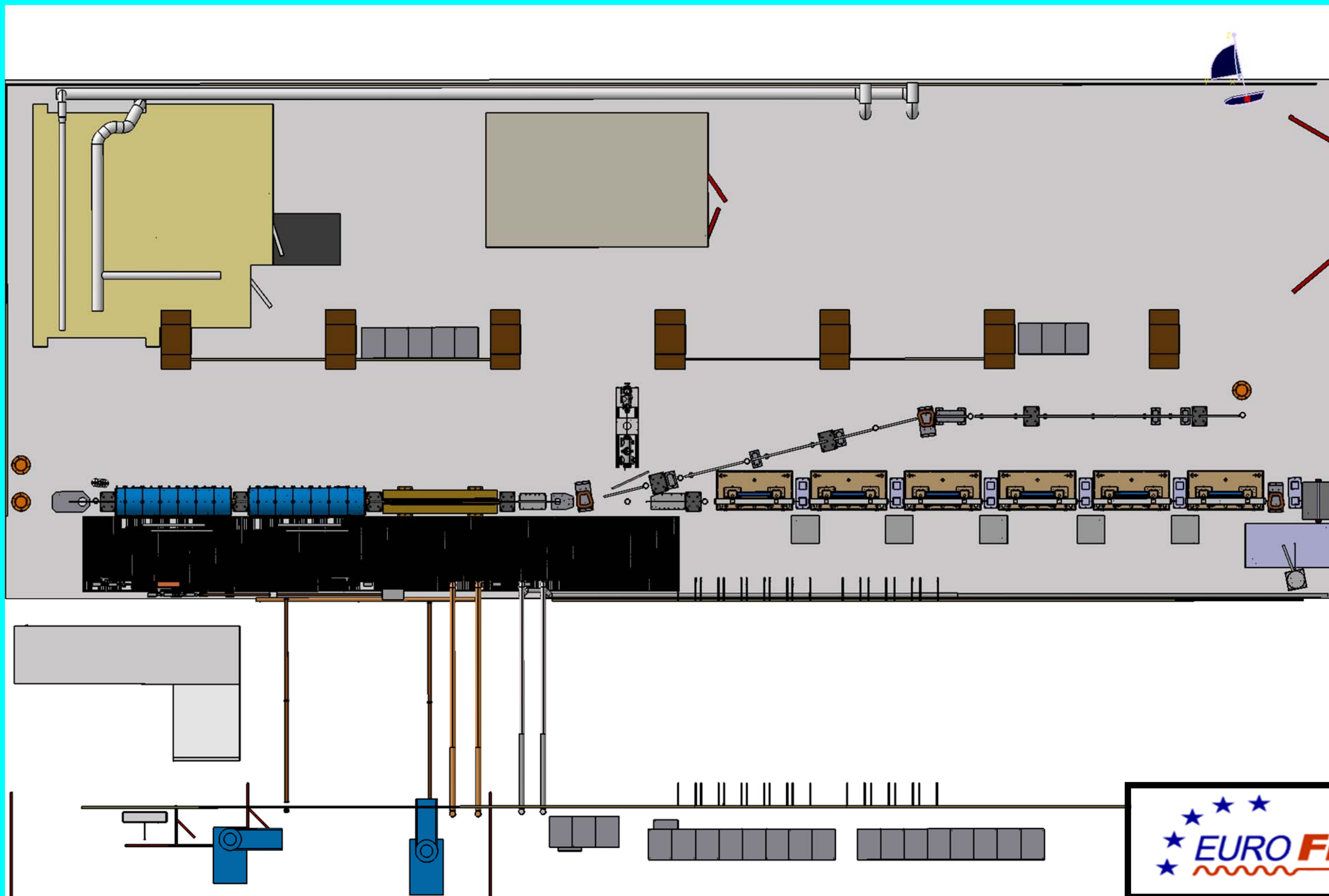

EURO FEL

Seeding @ SPARC

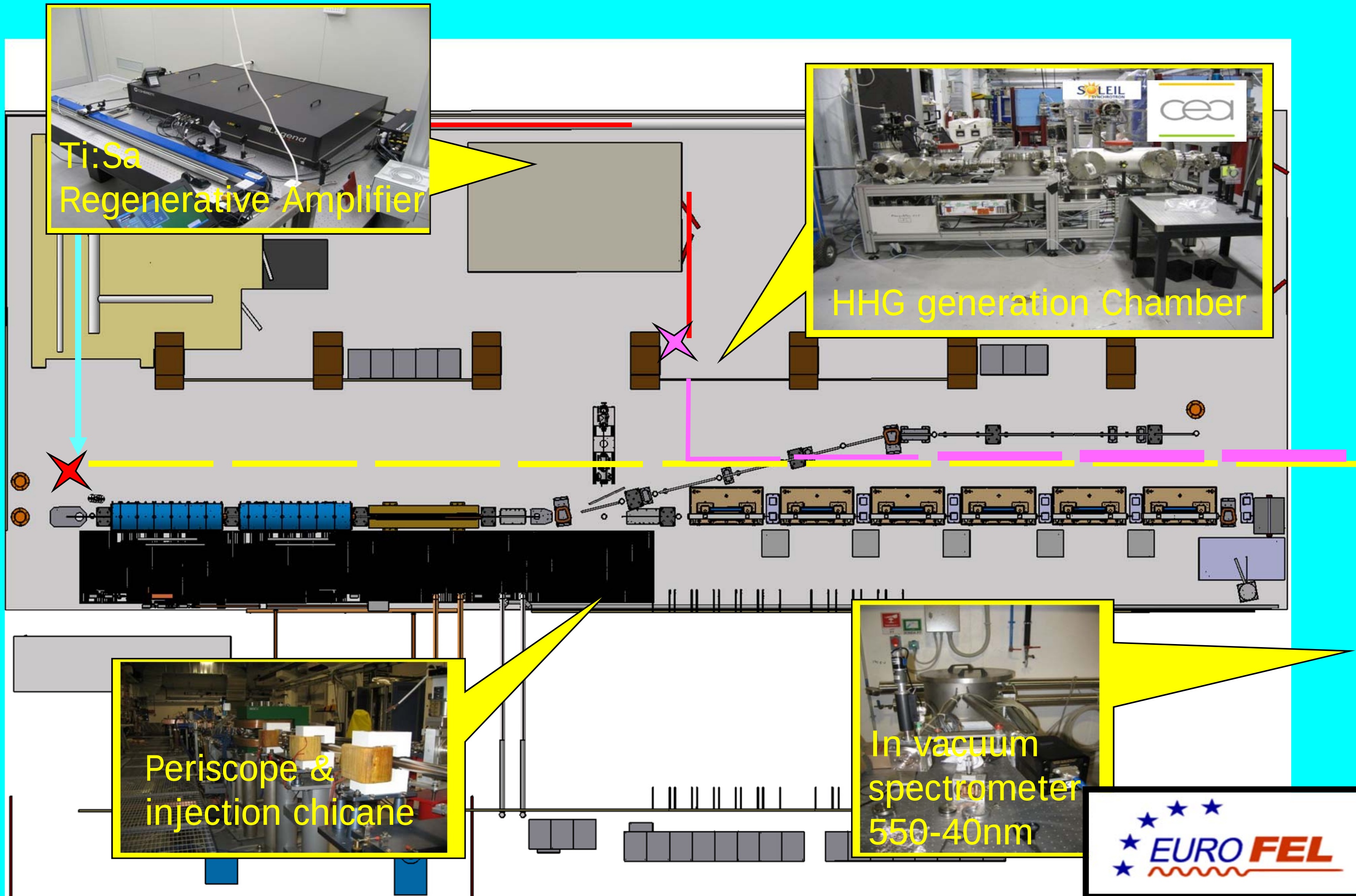

PRL **107,** 224801 (2011) PHYSICAL REVIEW LETTERS week ending 25 NOVEMBER 2011

High-Gain Harmonic-Generation Free-Electron Laser Seeded by Harmonics Generated in Gas

M. Labat,[1,9] M. Bellaveglia,[2] M. Bougeard,[11] B. Carré,[11] F. Ciocci,[1] E. Chiadroni,[2] A. Cianchi,[8,2] M. E. Couprie,[9] L. Cultrera,[2] M. Del Franco,[1] G. Di Pirro,[2] A. Drago,[2] M. Ferrario,[2] D. Filippetto,[2] F. Frassetto,[6] A. Gallo,[2] D. Garzella,[11] G. Gatti,[2] L. Giannessi,[1,*] G. Lambert,[12] A. Mostacci,[5] A. Petralia,[1] V. Petrillo,[3,4] L. Poletto,[6] M. Quattromini,[1] J. V. Rau,[7] C. Ronsivalle,[1] E. Sabia,[1] M. Serluca,[5] I. Spassovsky,[1] V. Surrenti,[1] C. Vaccarezza,[2] and C. Vicario[10]

- Seed an FEL cascade with harmonics generated in gas
- Study the evolution of the signal while varying the number of radiators/modulators

Seed λ_1 $\lambda_2 = \lambda_1/n,\ n=2$

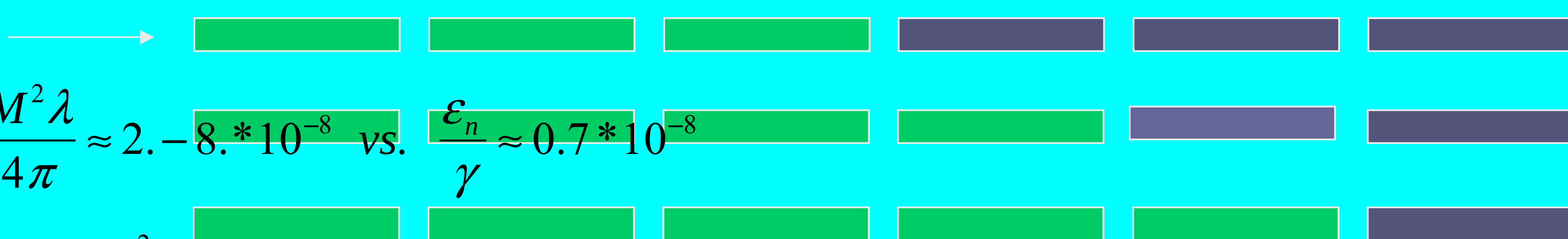

$$\frac{M^2\lambda}{4\pi} \approx 2.-8.*10^{-8} \quad vs. \quad \frac{\varepsilon_n}{\gamma} \approx 0.7*10^{-8}$$

$$Z_0 = \frac{\pi w_0^2}{\lambda} = 1.1 \quad m$$

Modulators Radiators

Seeding @ SPARC

SOLEIL SYNCHROTRON

cea

Seeding with harmonics generated in gas (Ar)

Ministero dell'Università e della Ricerca

EURO FEL

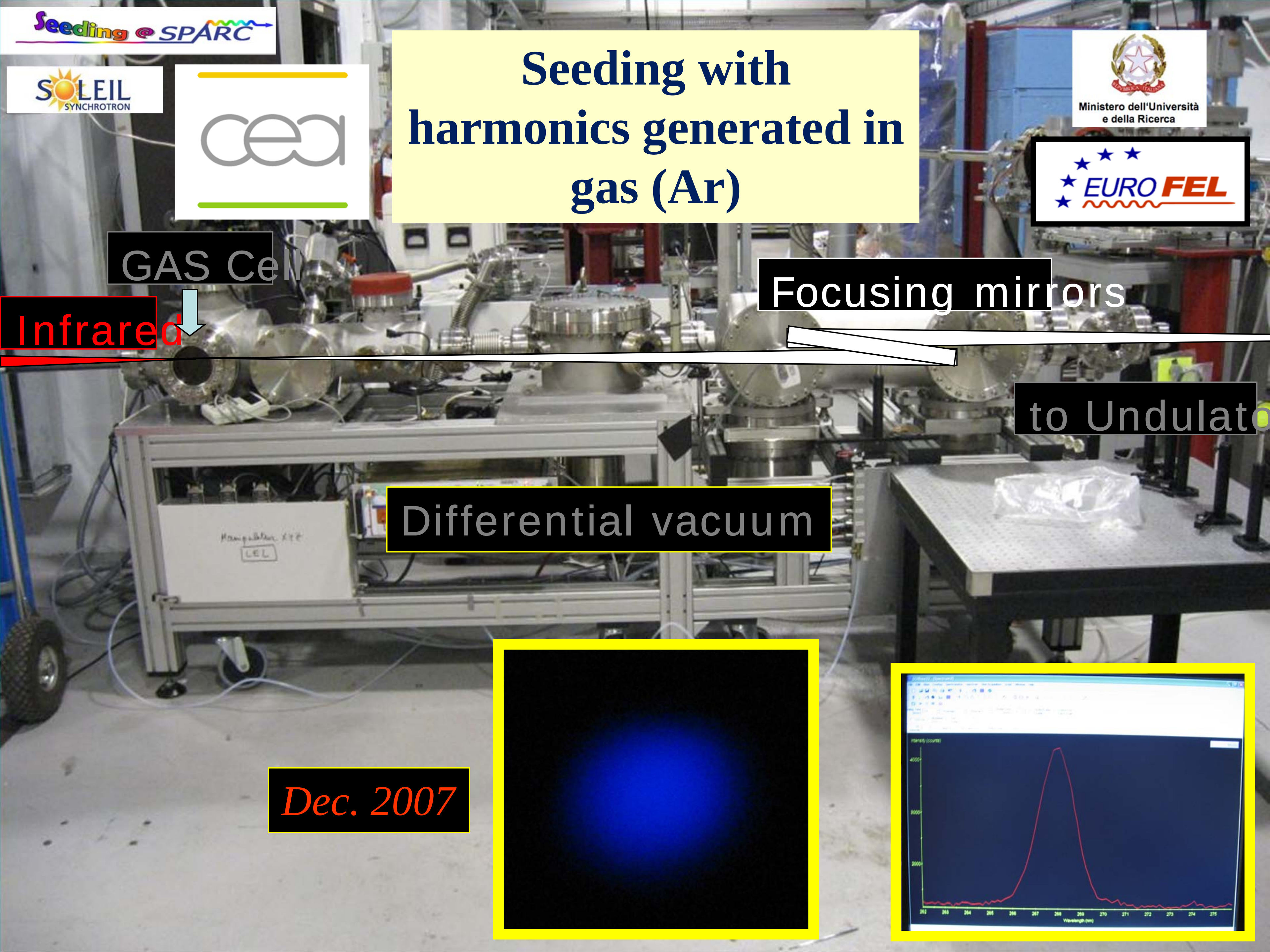
Seeding with harmonics generated in gas (Ar)
Seeding @ SPARC
SOLEIL SYNCHROTRON
cea
Ministero dell'Università e della Ricerca
EURO FEL
GAS Cell
Infrared
Focusing mirrors
to Undulato
Differential vacuum
Dec. 2007

Varying the number of radiators

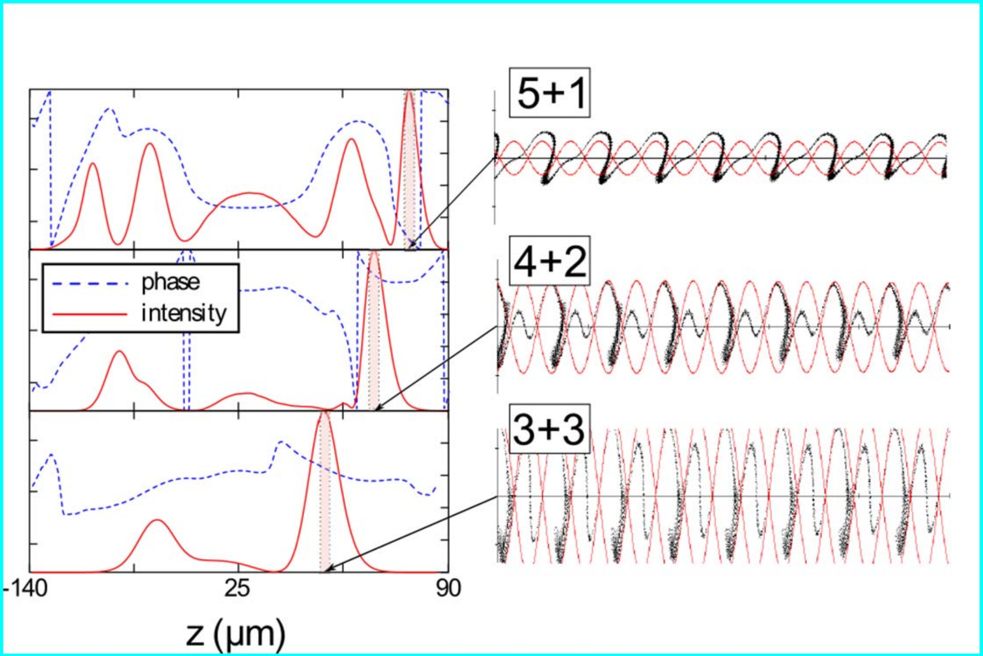

Transition from CHG to HGHG
Transfer the coherence of the seed to higher harmonics

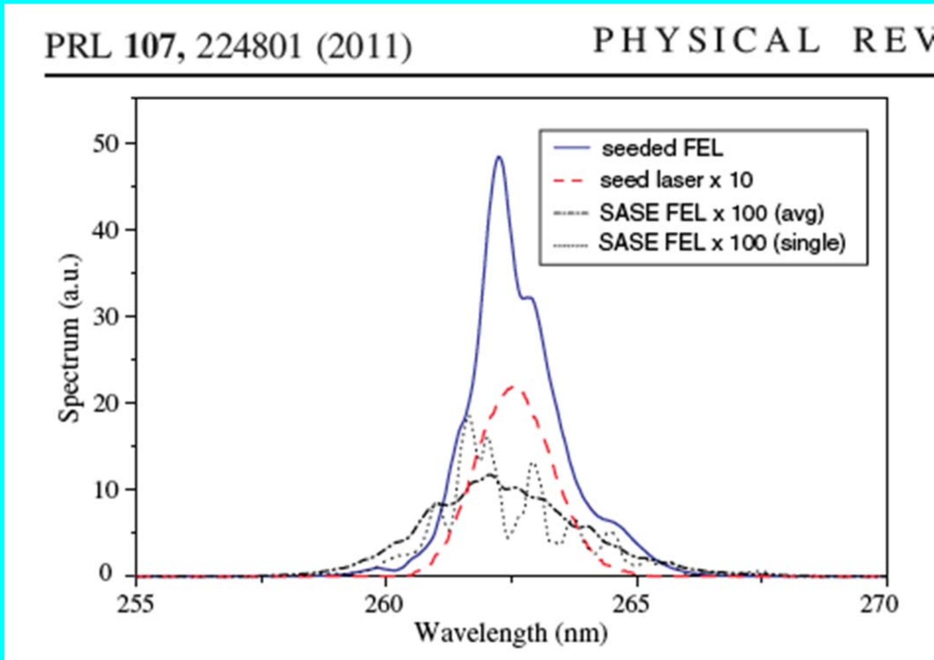

PRL **108,** 164801 (2012) PHYSICAL REVIEW LETTERS week ending 20 APRIL 2012

High-Order-Harmonic Generation and Superradiance in a Seeded Free-Electron Laser

L. Giannessi,[1,*] M. Artioli,[1] M. Bellaveglia,[2] F. Briquez,[9] E. Chiadroni,[2] A. Cianchi,[7] M. E. Couprie,[9] G. Dattoli,[1] E. Di Palma,[1] G. Di Pirro,[2] M. Ferrario,[2] D. Filippetto,[10] F. Frassetto,[5] G. Gatti,[2] M. Labat,[9] G. Marcus,[8] A. Mostacci,[4] A. Petralia,[1] V. Petrillo,[3] L. Poletto,[5] M. Quattromini,[1] J. V. Rau,[6] J. Rosenzweig,[8] E. Sabia,[1] M. Serluca,[4] I. Spassovsky,[1] and V. Surrenti[1]

- All the UM tuned at the same resonant wavelength (400nm)
- Induce superradiance by seeding the FEL amplifier at saturation intensity

Direct seeding

Superradiant regime @ 400 nm, <0.5 uJ – 9 uJ - 6 UM tuned at 400 nm

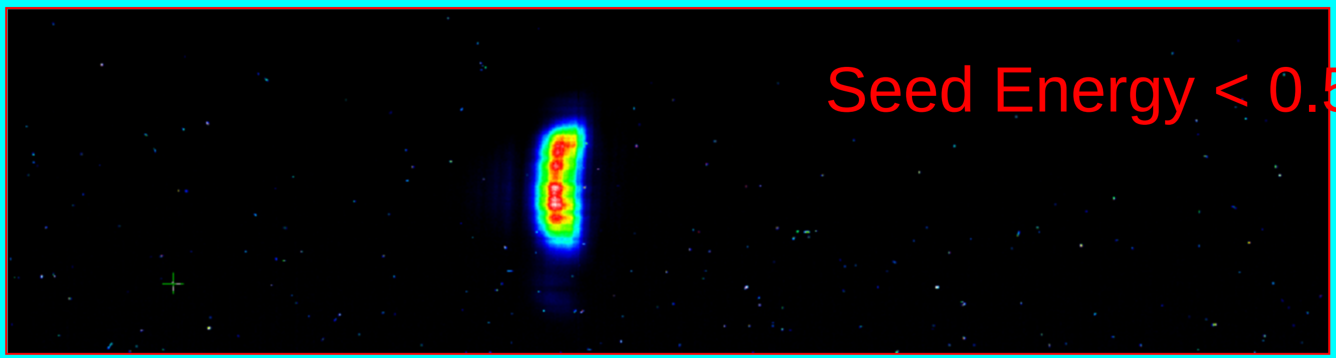

Seed Energy < 0.5 uJ

Direct seeding

Superradiant regime @ 400 nm, <0.5 uJ – 9 uJ - 6 UM tuned at 400 nm

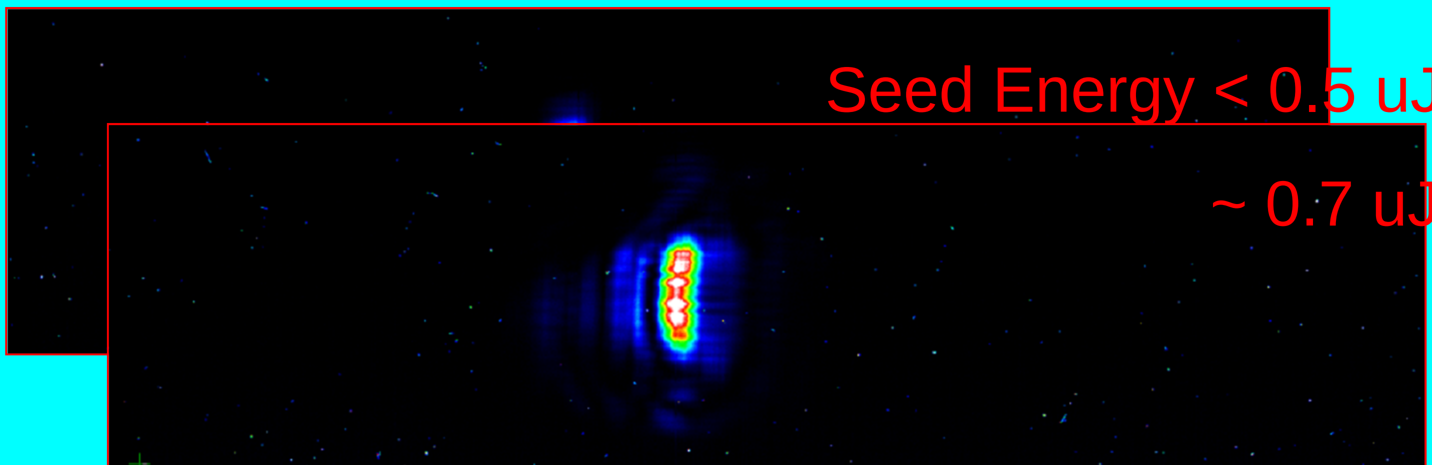

Direct seeding

Superradiant regime @ 400 nm, <0.5 uJ – 9 uJ - 6 UM tuned at 400 nm

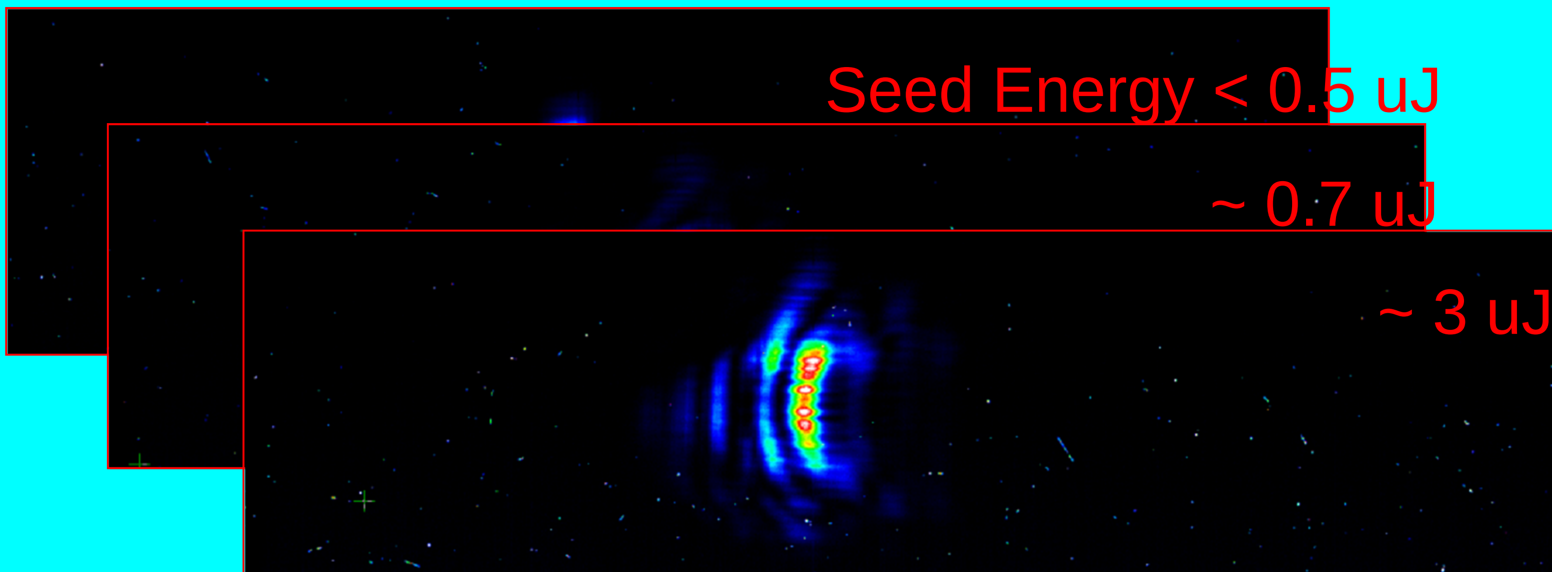

Direct seeding

Superradiant regime @ 400 nm, <0.5 uJ – 9 uJ - 6 UM tuned at 400 nm

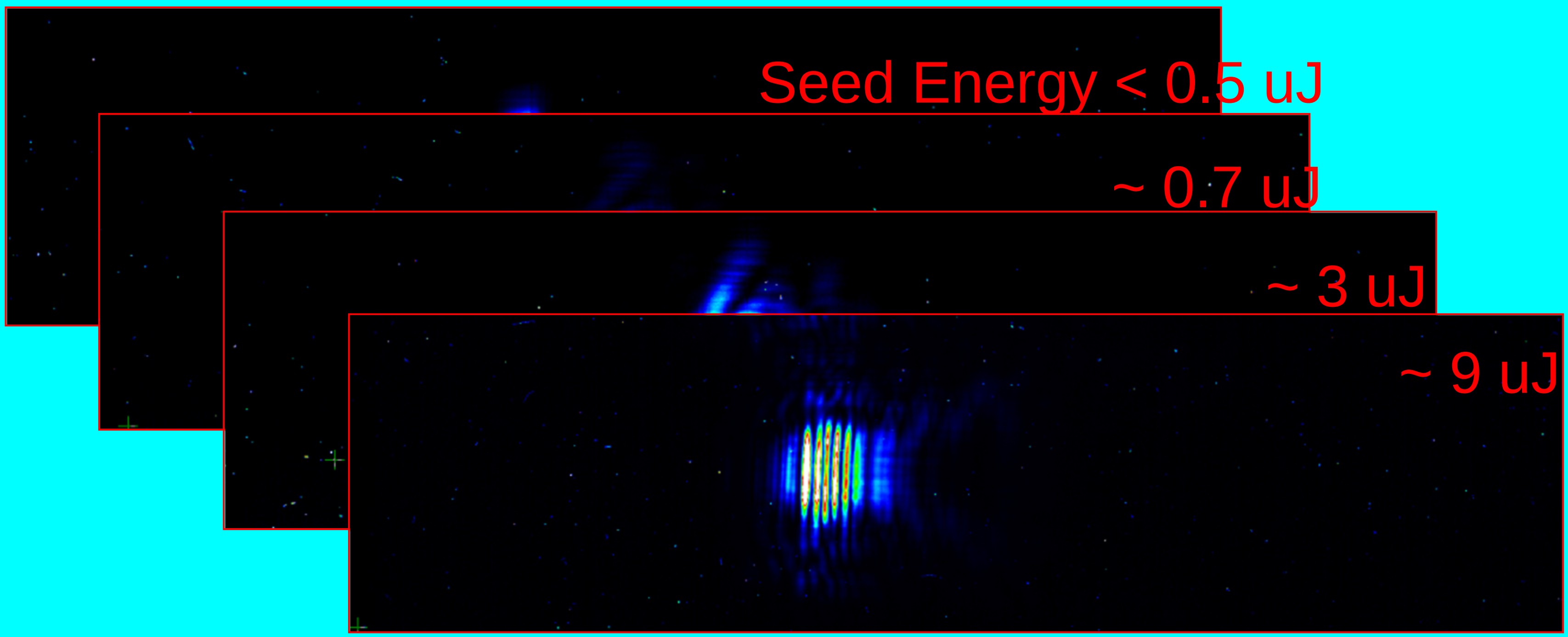

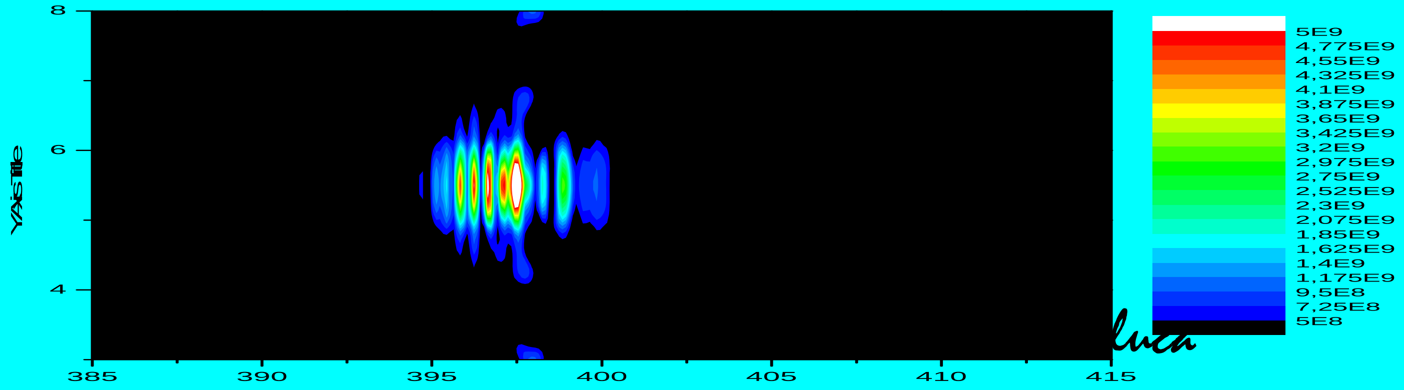

High harmonics down to 37 nm

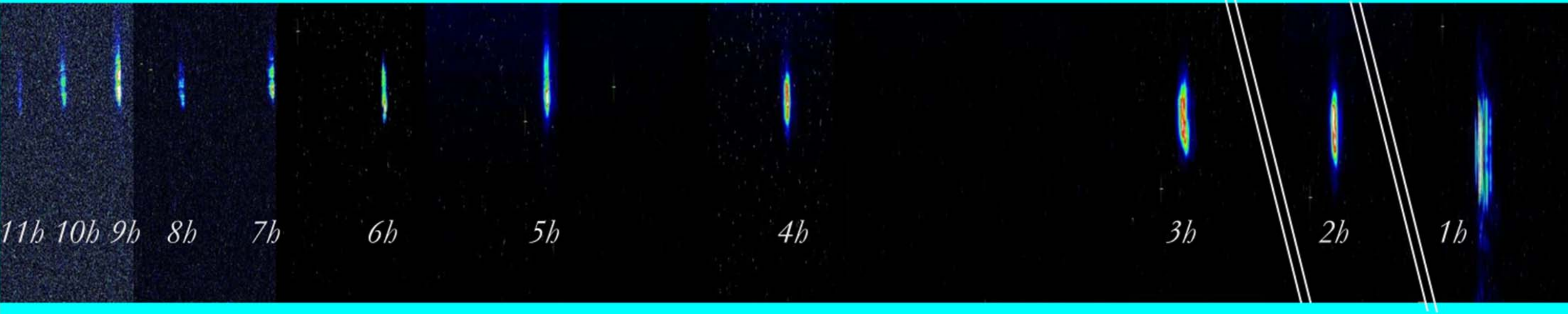

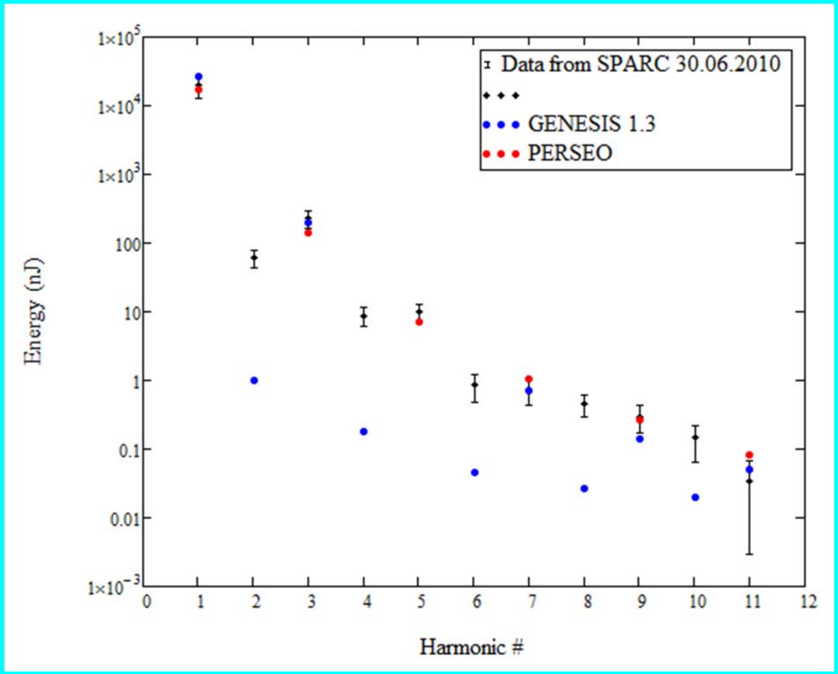

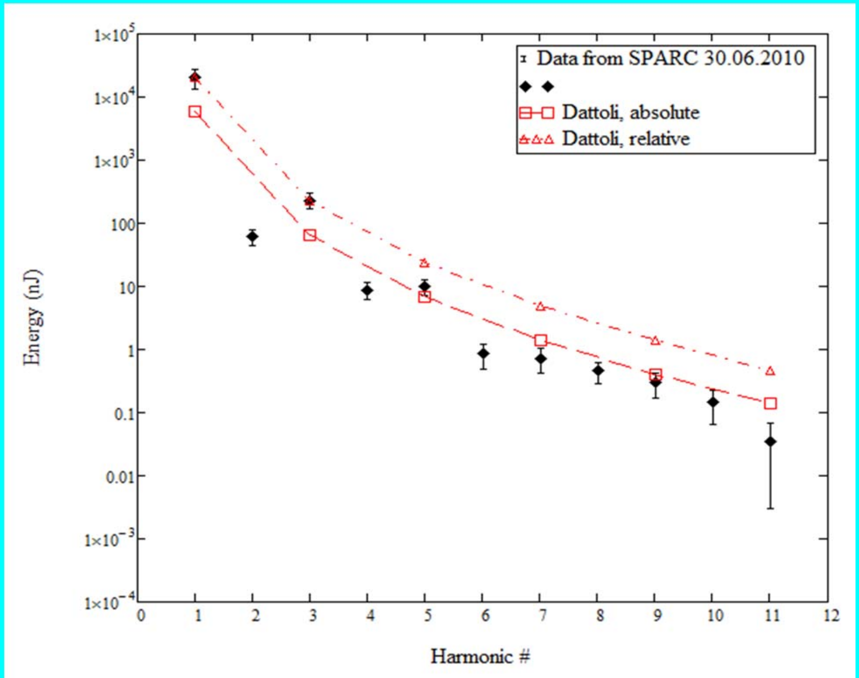

Measured energy per pulse, spot size & and bandwidth of the first 11° harmonics

INFN

SPARC_LAB

Other example of Coherence Transfer

Extreme ultraviolet free electron laser seeded with high-order harmonic of Ti:sapphire laser

Tadashi Togashi,[1,2] Eiji J. Takahashi,[3] Katsumi Midorikawa,[3] Makoto Aoyama,[4] Koichi Yamakawa,[4] Takahiro Sato,[1,5] Atsushi Iwasaki,[5] Shigeki Owada,[5] Tomoya Okino,[5] Kaoru Yamanouchi,[5] Fumihiko Kannari,[6] Akira Yagishita,[7] Hidetoshi Nakano,[8] Marie E. Couprie,[9] Kenji Fukami,[1,2] Takaki Hatsui,[1] Toru Hara,[1] Takashi Kameshima,[1] Hideo Kitamura,[1] Noritaka Kumagai,[1] Shinichi Matsubara,[1,2] Mitsuru Nagasono,[1] Haruhiko Ohashi,[1,2] Takashi Ohshima,[1] Yuji Otake,[1] Tsumoru Shintake,[1] Kenji Tamasaku,[1] Hitoshi Tanaka,[1,2] Takashi Tanaka,[1,2] Kazuaki Togawa,[1] Hiromitsu Tomizawa,[1,2] Takahiro Watanabe,[1,2] Makina Yabashi,[1] and Tetsuya Ishikawa[1]

[1]RIKEN, XFEL Project Head Office, Kouto 1-1-1, Sayo, Hyogo 679-5148, Japan
[2]Japan Synchrotron Radiation Research Institute, Kouto 1-1-1, Sayo, Hyogo 679-5198, Japan
[3]RIKEN Advanced Science Institute, Hirosawa 2-1, Wako, Saitama 351-0198, Japan
[4]Japan Atomic Energy Agency, Quantum Beam Science Directorate, Umemidai 8-1, Kizugawa, Kyoto 619-0215 Japan
[5]The University of Tokyo, Hongo 7-3-1, Bunkyo-ku, Tokyo 113-0033, Japan
[6]Keio University, Hiyoshi 3-14-1, Kohoku-ku Yokohama-shi, Kanagawa 223-8522, Japan
[7]KEK Photon Factory, Oho 1-1, Tsukuba, Ibaraki, 305-0801, Japan
[8]NTT Basic Research Laboratories, Morinosato 3-1, Atsugi, Kanagawa 243-019, Japan
[9]Synchrotron SOLEIL, L'Orme des Merisiers Saint-Aubin - BP 48 91192 Gif-sur-Yvette CEDEX, France

SPring8 Compact Sase Source (SCSS)

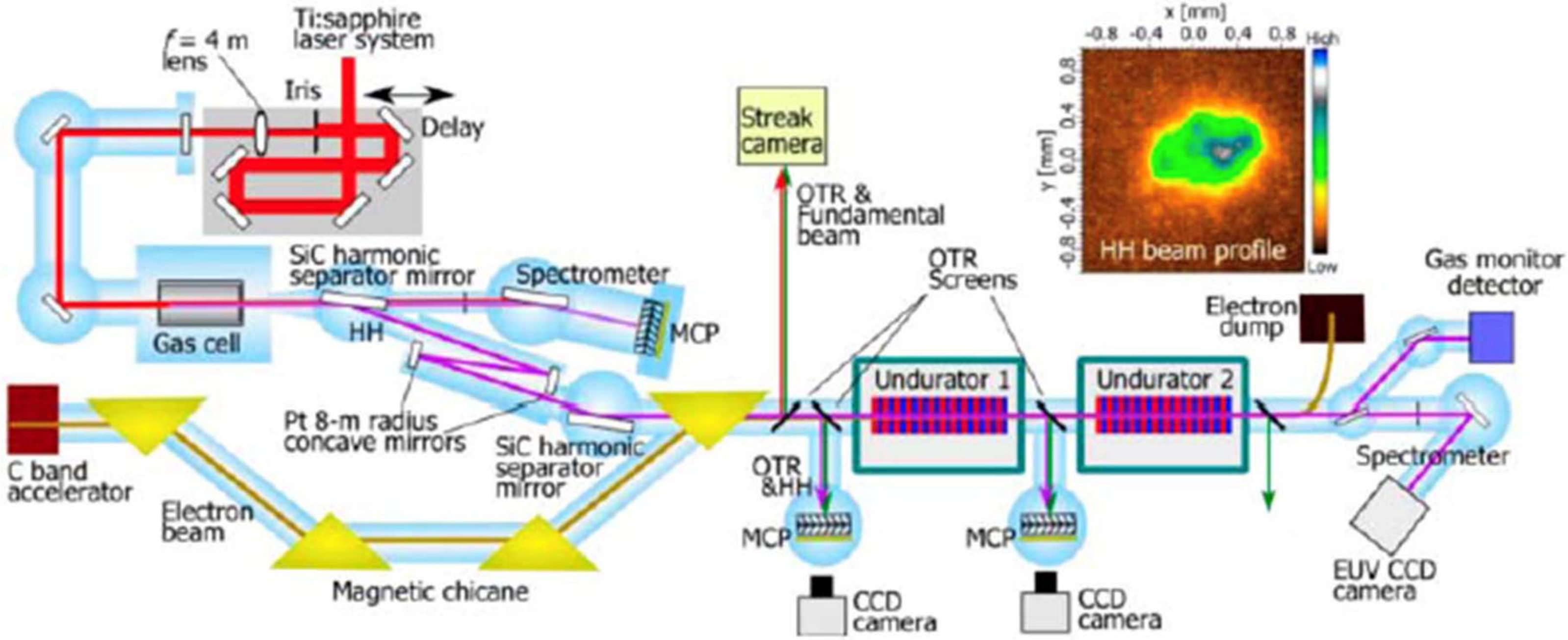

Fig. 1. Experimental setup. HH radiation is generated by loosely focusing a Ti:S laser (800 nm, 100 mJ, 160 fs FWHM, 30 Hz) in a Xe gas cell (focal length f = 4000 mm), and is separated from the fundamental beam by a SiC mirror. Pt-coated concave mirrors with 8000-mm radius of curvature are used for collimating and focusing HH radiation. The HH radiation is transported by the SiC mirror to the undulator section, overlapped with an electron beam (250 MeV, 300 fs, 30 Hz) spatially and temporally. The seeded FEL is observed by the spectrometer at the end of the beamline. The inset shows the beam profile of HH radiation at the undulator entrance. The spatial profile was measured by a phosphor screen coupled with a multichannel plate (MCP) and CCD camera.

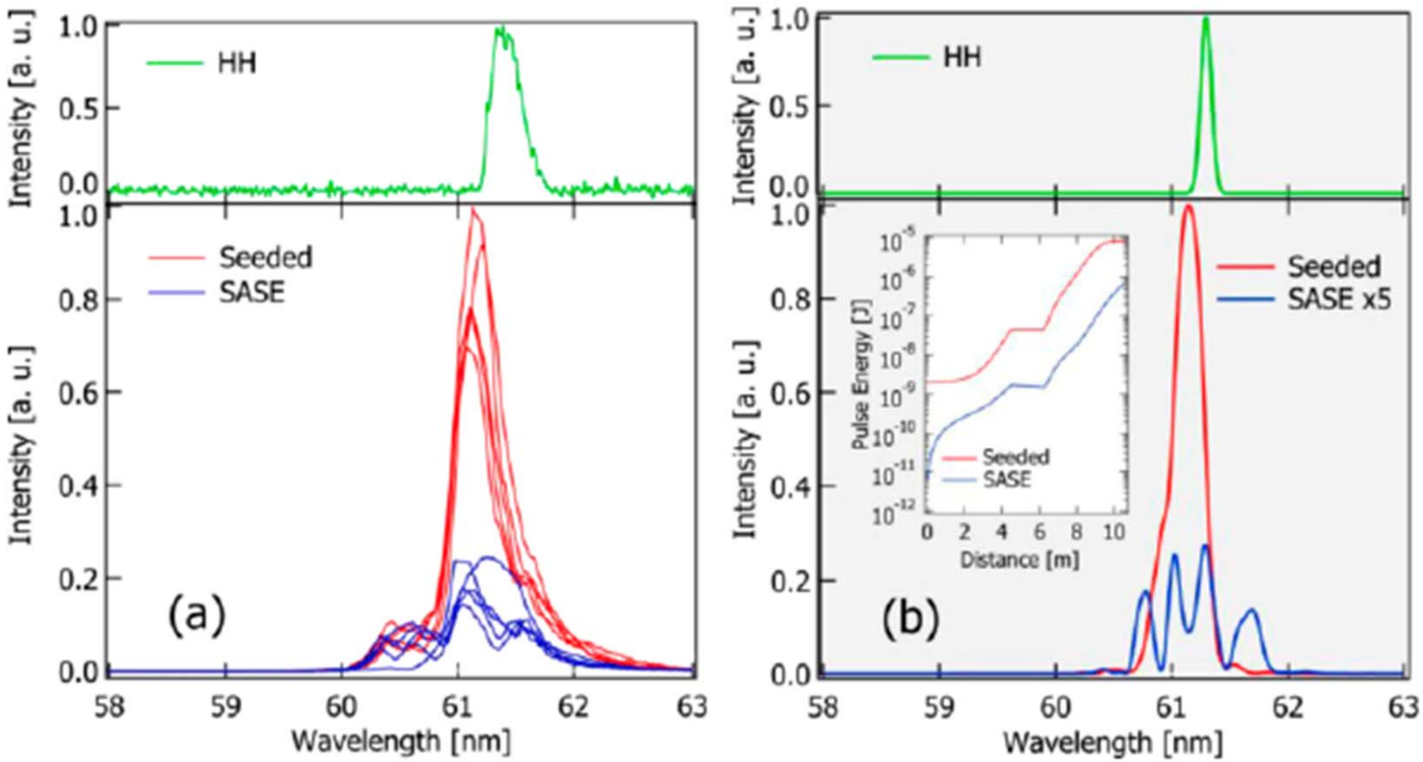

Fig. 3. Spectra of seeded (red lines) and unseeded (blue lines) conditions, as well as that of HH radiation (green line), given by experiment (a) and simulation (b). The inset of (b) shows intensity growths along the undulator for seeded (red line) and unseeded (blue line) conditions.

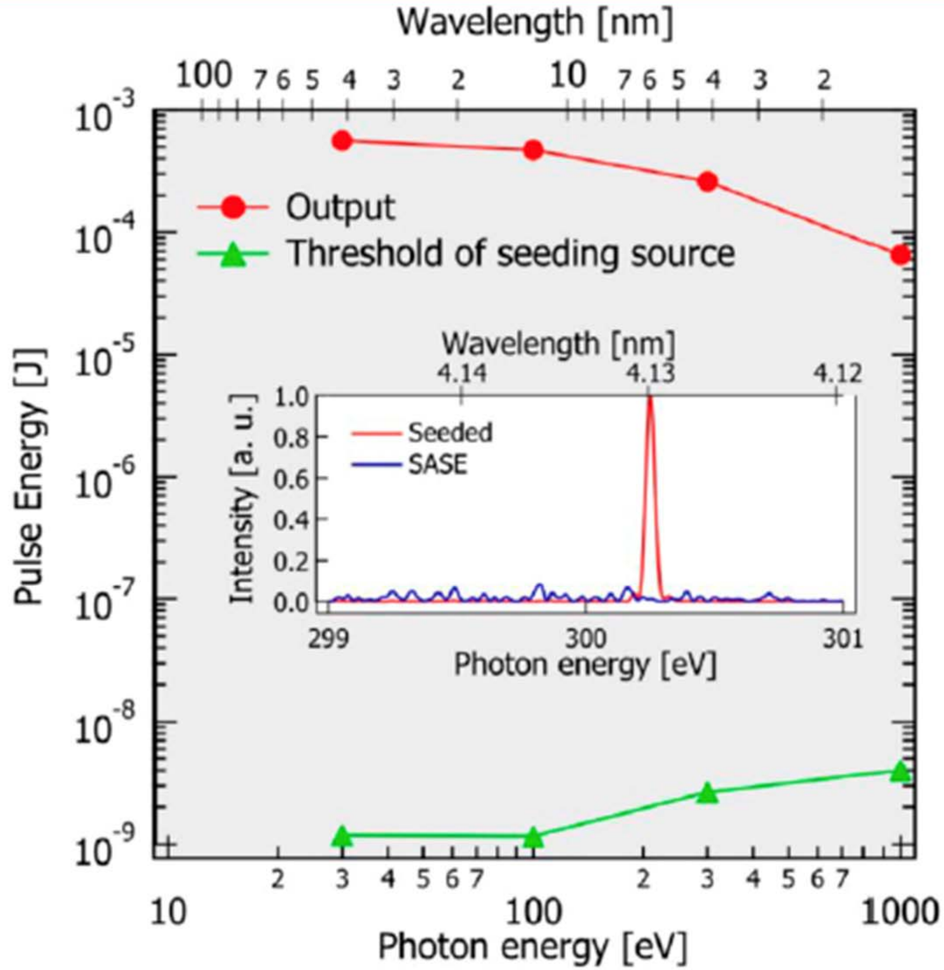

Fig. 4. The intensity threshold of the seeding source (green line) and output intensity after FEL amplification (red line), as a function of photon energy (lower axis) and wavelength (upper axis). The inset shows the simulated spectra of the seeded (red line) and the unseeded (blue line) conditions at a wavelength of 4 nm. The intensity of HH radiation, 2.6 nJ/pulse, corresponds to the threshold level required for operating seeded FEL.

Marrying Lasers and Particle Beams

Inverse Free Electron Laser: transfer energy from the Laser to the Electron Beam through the FEL radiation

IFEL Interaction

In an FEL energy in the e-beam is transferred to a radiation field

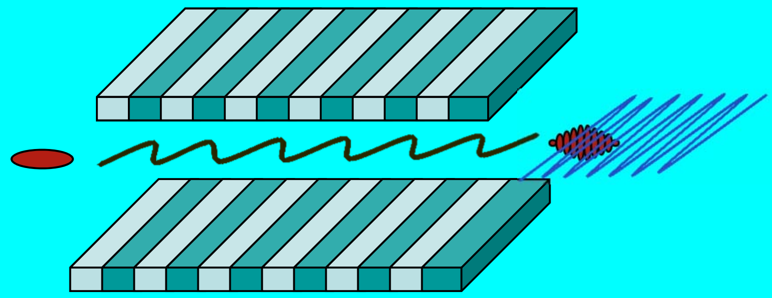

In an IFEL the electron beam absorbs energy from a radiation field.

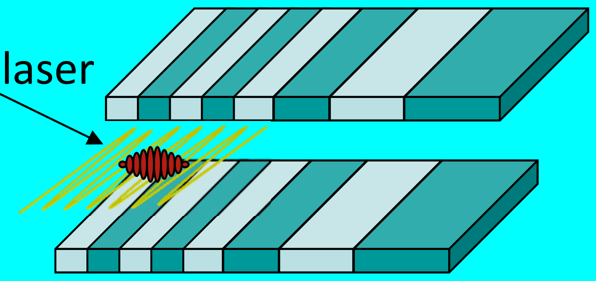

Undulator magnetic field to couple high power radiation with relativistic electrons

$$K_l = \frac{eE_0}{mc^2 k} \qquad K = \frac{eB}{mck_w}$$

$$\boxed{\gamma_r^{\,2} \cong \frac{\lambda_w}{2 \cdot \lambda} \cdot \left(1 + \frac{K^2}{2}\right)}$$

Significant energy exchange between the particles and the wave happens when the resonance condition is satisfied.

Useful scalings for IFEL accelerator

Assuming no guiding and a single stage helical undulator

The ideal relationship between the Rayleigh range and the total undulator length is

$$L_u \approx 6\ z_r$$

⇩ A tight focus increases the intensity, but only in one spot.

⇧ A large z_r maximizes the gradient over entire undulator length

$$\frac{M^2\lambda}{4\pi} \approx 8.*10^{-8} \quad vs. \quad \frac{\varepsilon_n}{\gamma_{in}} \approx 1.*10^{-8} \quad and \quad \frac{\varepsilon_n}{\gamma_{fin}} \approx 5.*10^{-10}$$

Final energy (assuming a const. K, or taking the average value for K) will be given by

$$\Delta\gamma^2 \cong 12\sqrt{2}\,\frac{e_0\sqrt{Z_0}}{mc^2}\sqrt{\frac{z_r}{\lambda}}\sqrt{P}\,\overline{K} \cong 6\cdot 10^{-4}\sqrt{\frac{z_r}{\lambda}}\sqrt{P(W)}\,\overline{K}$$

In order to have the final energy 500 MeV ($\gamma_f^2 = 10^6$) with a 1 (0.8)um laser, z_r = 15 cm and K ~ 4 The laser power P needs to be 5 TW or higher

Beam loading

Take as an example the case of a 1 GeV accelerator
The laser power P needs to be 20 TW or higher

4 J in 200 fs   20 J in 1 ps   100 J in 4 ps

Slippage problem.
Pulse length / optical period has to be larger than number of periods in undulator.

Energy is linear with accelerated charge

1000 MeV x 100 pC = 0.1 J
1000 MeV x 1 nC = 1 J

Need to choose laser pulse length/energy based on these considerations.

From proof-of-principle to 2nd generation IFEL experiments

- Proof-of-principle experiments successful
- Upgrade to significant gradient and energy gain
  - Technical challenges:
    - staging
    - very high power radiation
    - strong undulator tapering
  - Physics problems:
    - microbunching preservation
    - include diffraction effects in the theory
    - beyond validity of period-averaged classical FEL equation

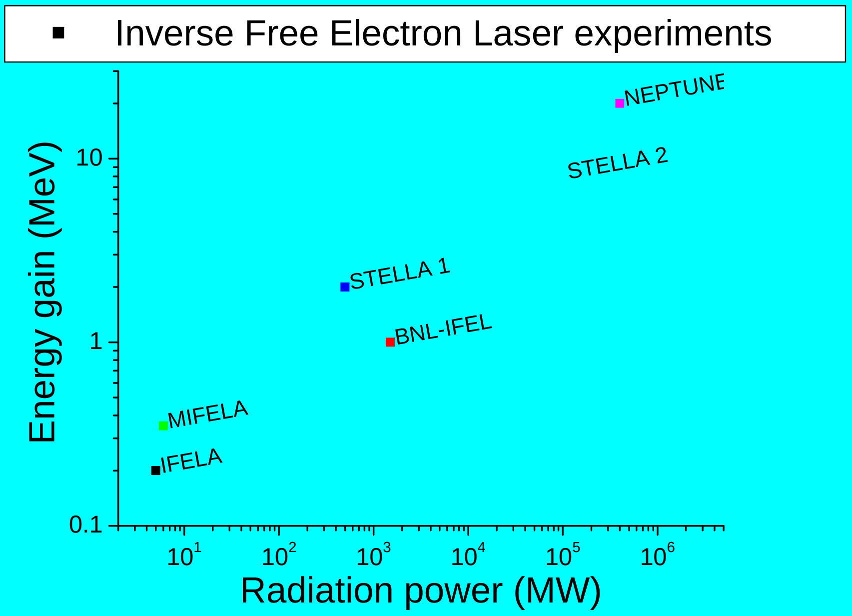

Cryogenic undulator + 20 TW laser power "green-field" design

If gap is maintained large one can adopt a fully permanent magnet design (no iron poles)

Optimization keeping resonant phase at 45 degrees
Compromise between capture and gradient
6 mm gap

Initial energy	50 MeV
Final energy	1200 MeV
Avg gradient	1.1 GV/m
Final energy spread	1 %
Laser wavelength	800 nm
Laser power	20 TW
Laser spot size (w_0)	0.2 mm

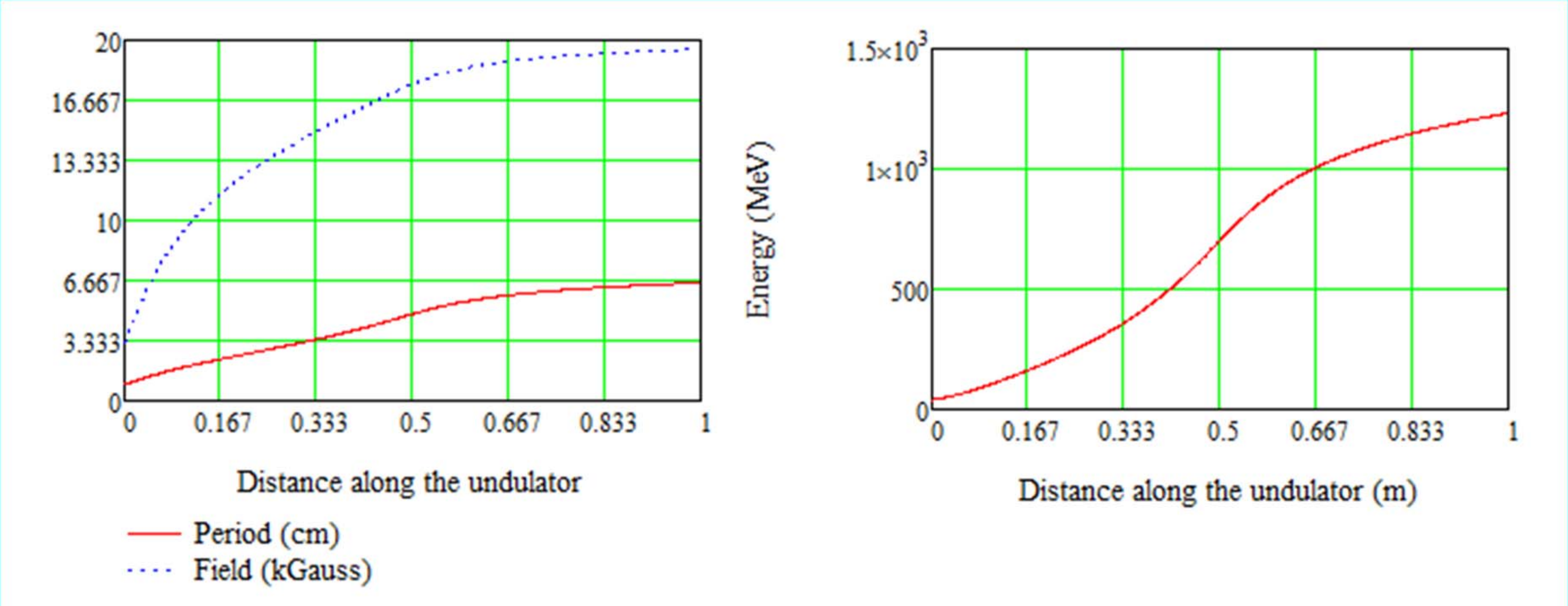

High Gradient High Energy Gain Inverse Free Electron Laser

P. Musumeci et al.

- Renovated interest in IFEL acceleration scheme
- Applications as compact scheme to obtain 1-2 GeV electron beam for gamma ray (ICS) or soft x-ray (FEL) generation.

Radiabeam UCLA BNL IFEL Collaboration

Strongly tapered optimized helical permanent magnet undulator

ATF @ BNL
0.5 TW CO2 laser
50 MeV -> 180 MeV in 60 cm
130 MeV energy gain
220 MV/m gradient

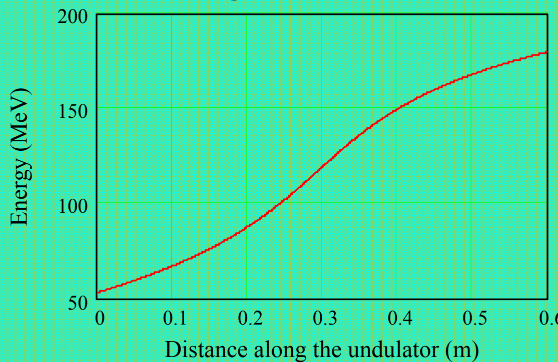

LLNL-UCLA IFEL experiment

Reuse UCLA- Kurchatov undulator

Use 5 TW 10 Hz Ti:Sa
50 MeV -> 150 MeV in 50 cm

High rep rate allows beam quality measurement

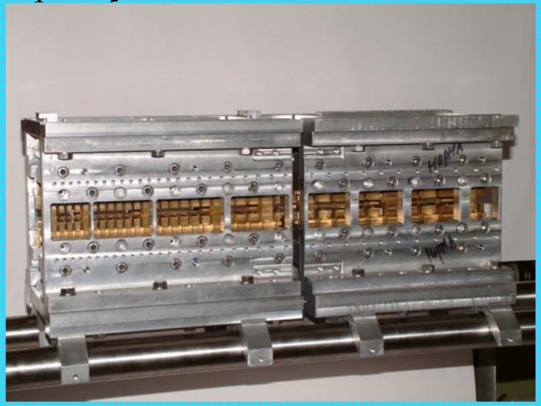

GeV IFEL experiment

If current experiments succesfull

Looking for access to facility with 50 MeV beam+20 TW laser (BNL, LLNL, LNF-Italy)

Praesodymium based cryogenic undulator

Initial energy	50 MeV
Final energy	1200 MeV
Avg gradient	1.1 GV/m
Final energy spread	1 %
Laser wavelength	800 nm
Laser power	20 TW
Laser spot size (w_0)	0.2 mm

Marrying Lasers and Particle Beams

Inverse Compton Scattering:
the Photon Accelerator
frequency Doppler/Lorentz upconversion by the Electron Beam of the Laser Photons

where the phase space densities of the two colliding beams are mapped into the gamma photon beam

Beams of γ, not just one photon per shot

Classical model

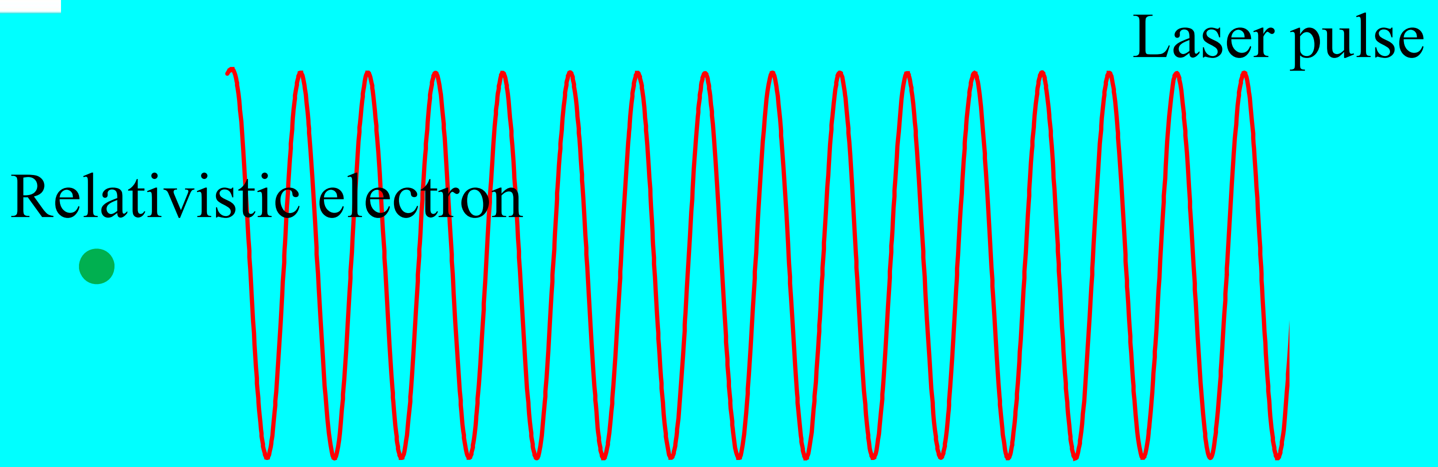

Classical model

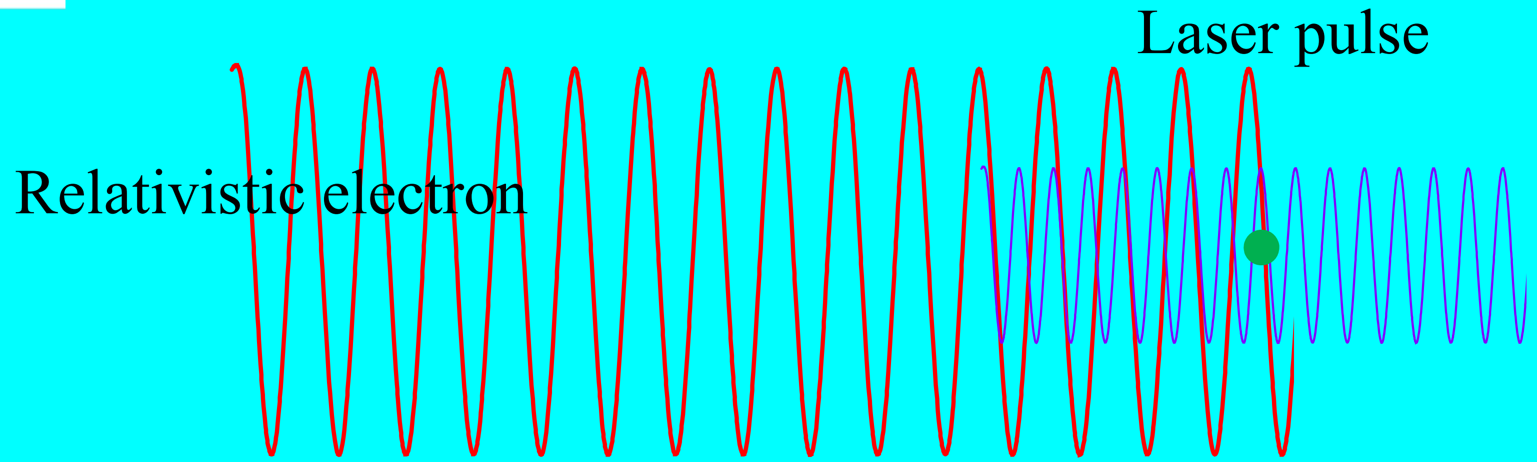

Classical model

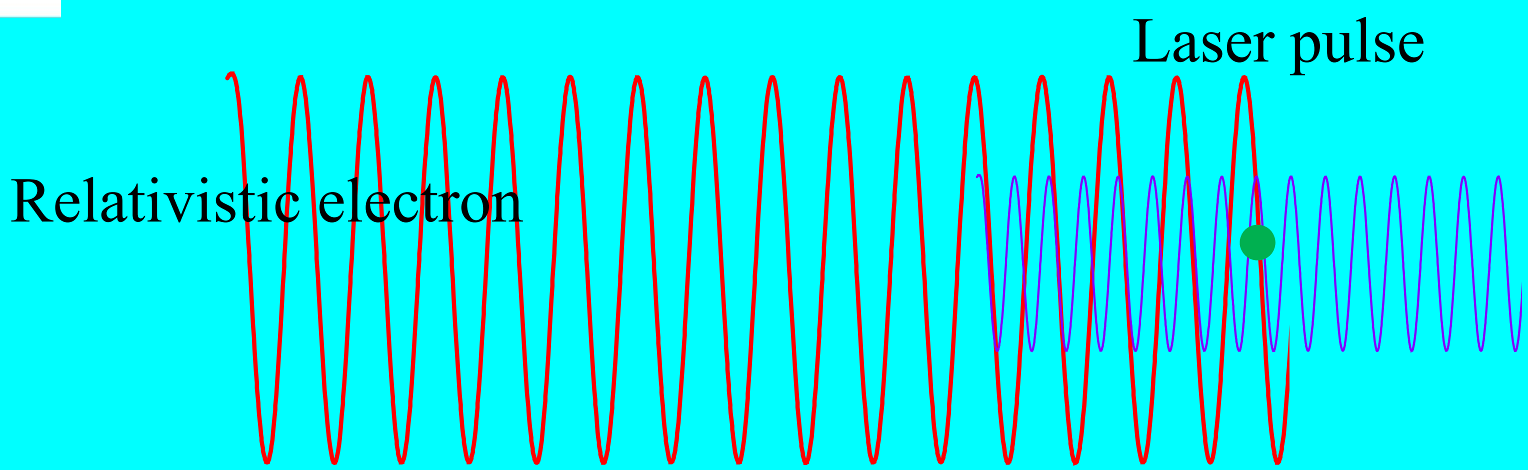

From the double Doppler effect :

$$\nu = \nu_L \frac{1-\underline{e}_k \cdot \underline{\beta}_0}{1-\underline{n}\cdot\underline{\beta}_0} \approx 4\gamma^2 \nu_L$$

$$\lambda = \lambda_L \frac{1-\underline{n}\cdot\underline{\beta}_0}{1-\underline{e}_k \cdot \underline{\beta}_0}$$

Head-on scattering $\lambda = \lambda_L \dfrac{1}{4\gamma_0^{\,2}}$
Radiation on axis

$$\frac{M^2\lambda}{4\pi} \approx 8.*10^{-8} \quad vs. \quad \frac{\varepsilon_n}{\gamma}[Thomson] \approx 5.*10^{-8} \quad and \quad \frac{\varepsilon_n}{\gamma}[Compton] \approx 5.*10^{-10}$$

Classical double differential spectrum

From the electron orbits and the Liénard-Wiechert far zone the expression to calculate the radiation field [Jackson..] for **one electron** is:

$$\frac{d^2W_i}{d\omega d\Omega} = \frac{e^2}{4\pi^2 c}\left|\int_{-\infty}^{+\infty} dt e^{i\omega t}\,\frac{\mathbf{n}\times\left[(\mathbf{n}-\beta(t'))\times\dot{\beta}(t')\right]}{(1-\mathbf{n}\cdot\beta(t'))^3}\right|^2 = \hbar\omega\frac{\mathrm{d}^2\mathrm{N}_\mathrm{i}}{\mathrm{d}\omega\mathrm{d}\Omega}$$

And for all the beam:

$$\hbar\omega\frac{\mathrm{d}^2\mathrm{N}}{\mathrm{d}\omega\mathrm{d}\Omega} = \hbar\omega\sum_i\frac{\mathrm{d}^2\mathrm{N}_\mathrm{i}}{\mathrm{d}\omega\mathrm{d}\Omega}$$

The previous expressions are at the basis of the semi-analytical classical non linear code **TSST**

P. Tomassini et al., IEEE TRANSACTIONS ON PLASMA SCIENCE, VOL. 36, NO. 4, AUGUST 2008

Quantum model

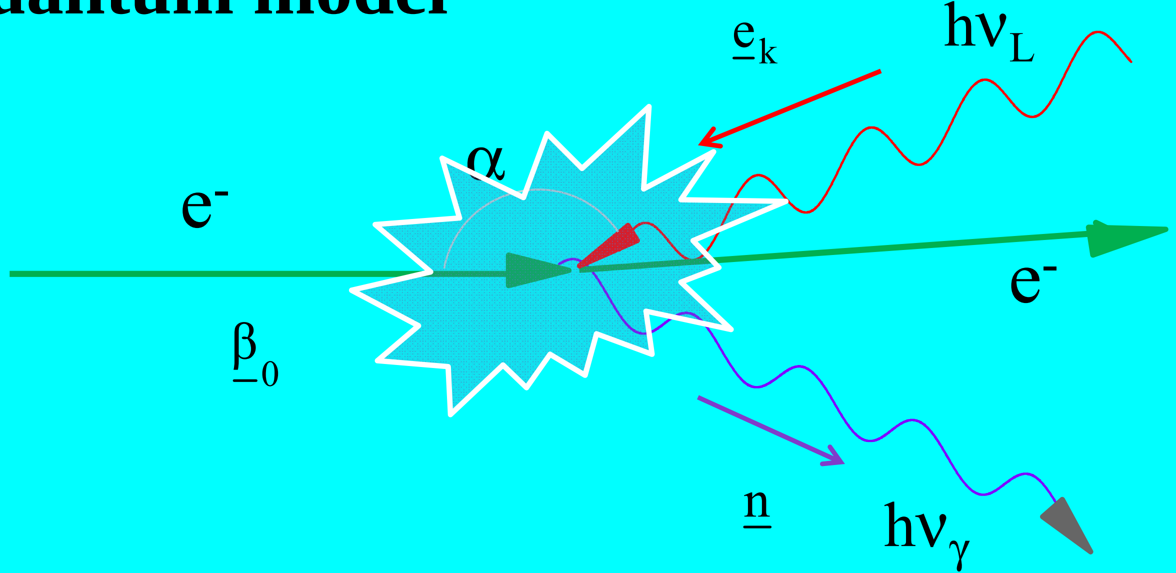

$$mc^2(\gamma-\gamma_0)=-h(\nu-\nu_L)$$

$$mc(\underline{\beta}\gamma-\underline{\beta}_0\gamma_0)=-h(\underline{k}-\underline{k}_L)/2\pi$$

Energy and momentum conservation laws

γ_0:initial Lorentz factor

$$\nu = \nu_L \frac{1-\underline{e}_k\cdot\underline{\beta}_0}{1-\underline{n}\cdot\underline{\beta}_0 + \boxed{\frac{h\nu_L}{mc^2\gamma_0}(1-\underline{e}_k\cdot\underline{n})}}$$

$$\lambda = \boxed{\lambda_L \frac{1-\underline{n}\cdot\underline{\beta}_0}{1-\underline{e}_k\cdot\underline{\beta}_0}} + \boxed{\frac{h}{mc\gamma_0}\frac{1-\underline{e}_k\cdot\underline{n}}{1-\underline{e}_k\cdot\underline{\beta}_0}}$$

Back-scattering
Radiation on-axis

$$\lambda = \boxed{\lambda_L \frac{1}{4\gamma_0^2}} + \boxed{\frac{h}{mc\gamma_0}}$$

Thomson factor

Compton red shift

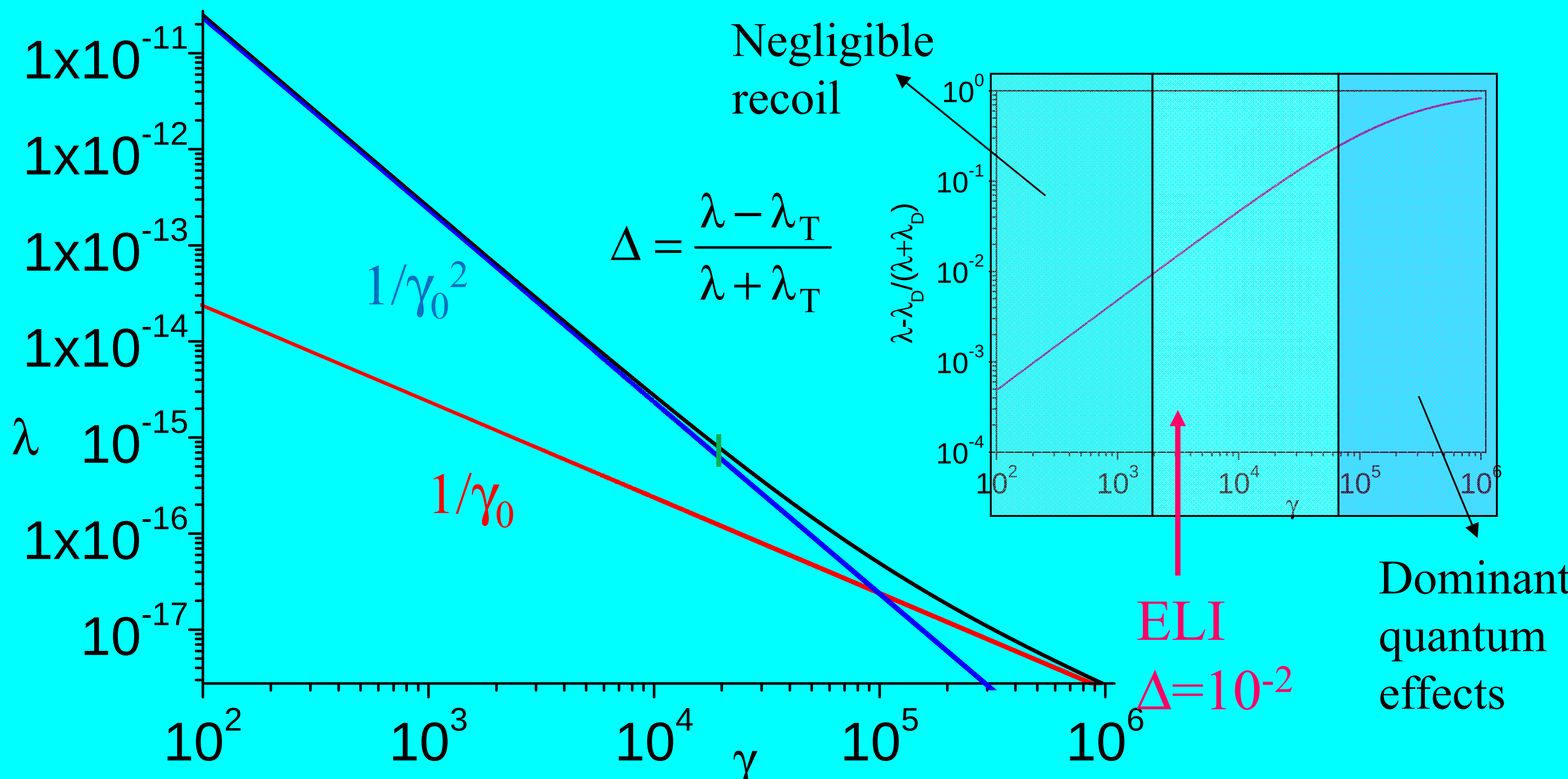

Angle-frequency correlation

$$\nu = \nu_L \frac{1-\underline{e}_k \cdot \underline{\beta}_0}{1-\underline{n}\cdot\underline{\beta}_0 + \dfrac{h\nu_L}{mc^2\gamma_0}\left(1-\underline{e}_k \cdot \underline{n}\right)}$$

Collecting the radiation in an acceptance angle $\theta \gg 1/\gamma$, the spectrum is white.

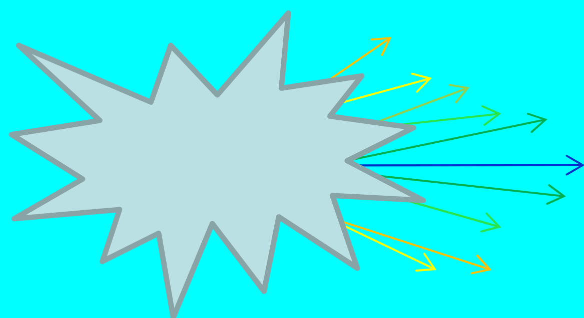

CAIN results

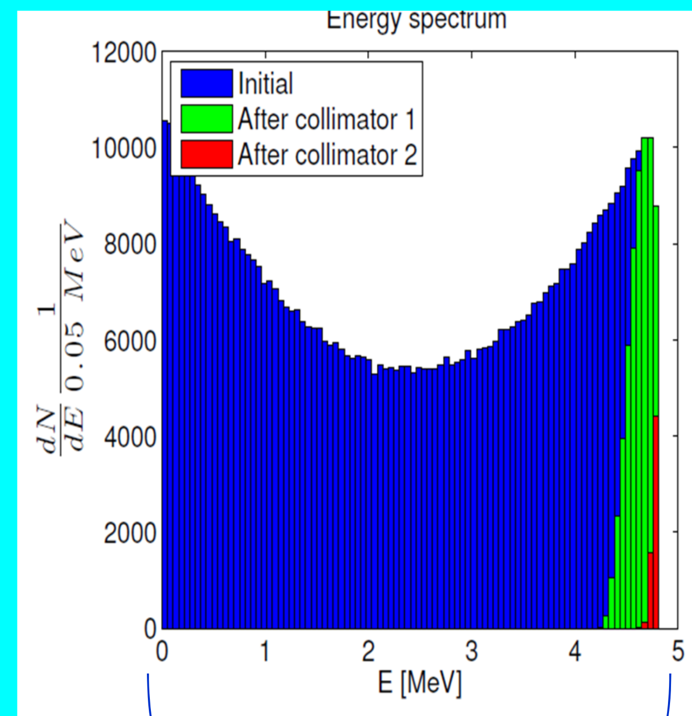

The most energetic photons are emitted on or close to the axis

White spectrum

I.Chaikovska and A. Variola

Angle-frequency correlation

$$\nu = \nu_L \frac{1-\underline{e}_k\cdot\underline{\beta}_0}{1-\underline{n}\cdot\underline{\beta}_0+\dfrac{h\nu_L}{mc^2\gamma_0}\left(1-\underline{e}_k\cdot\underline{n}\right)}$$

Collecting the radiation in an acceptance angle $\theta >> 1/\gamma$, the spectrum is white.

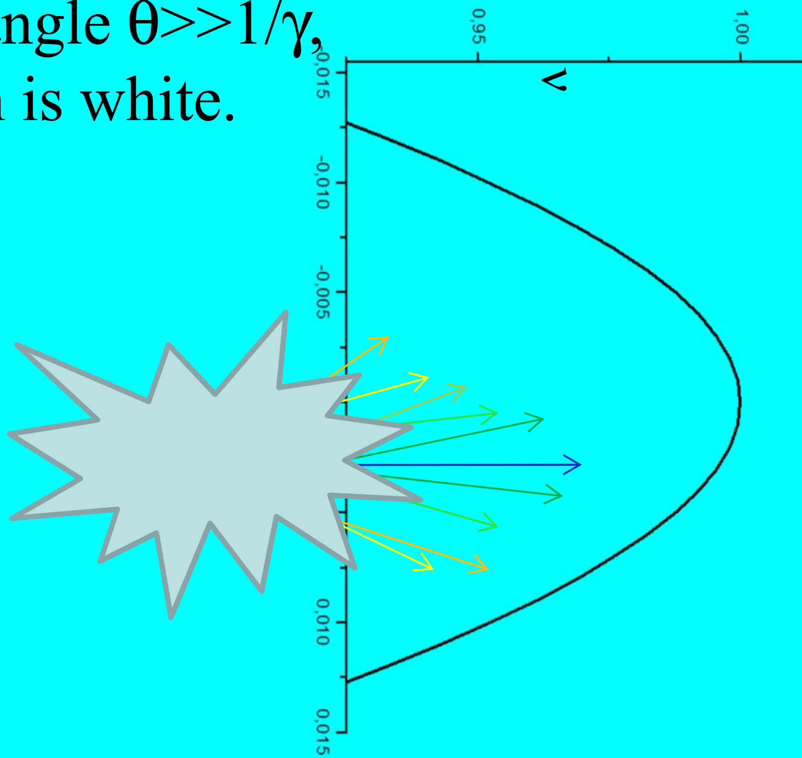

CAIN results

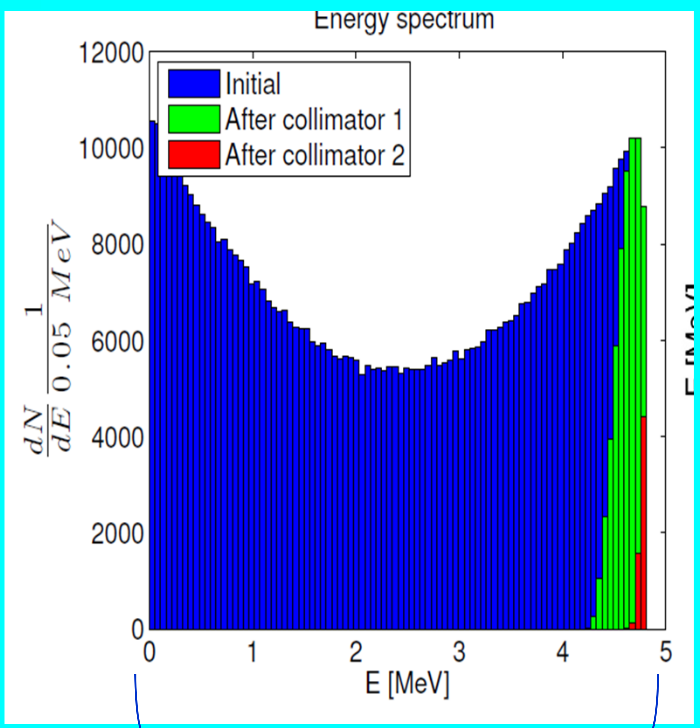

The most energetic photons are emitted on or close to the axis

White spectrum

I.Chaikovska and A. Variola

Angle-frequency correlation

$$\nu = \nu_L \frac{1-\underline{e}_k \cdot \underline{\beta}_0}{1-\underline{n}\cdot\underline{\beta}_0 + \frac{h\nu_L}{mc^2\gamma_0}(1-\underline{e}_k\cdot\underline{n})}$$

Collecting the radiation in an acceptance angle $\theta >> 1/\gamma$, the spectrum is white.

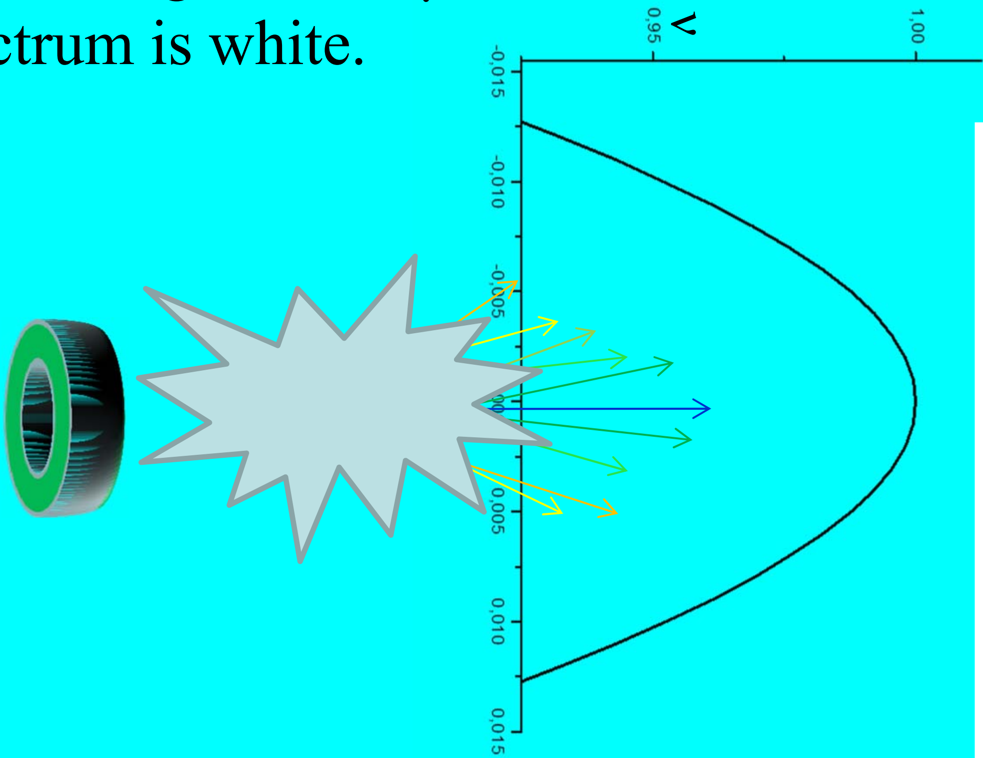

CAIN results

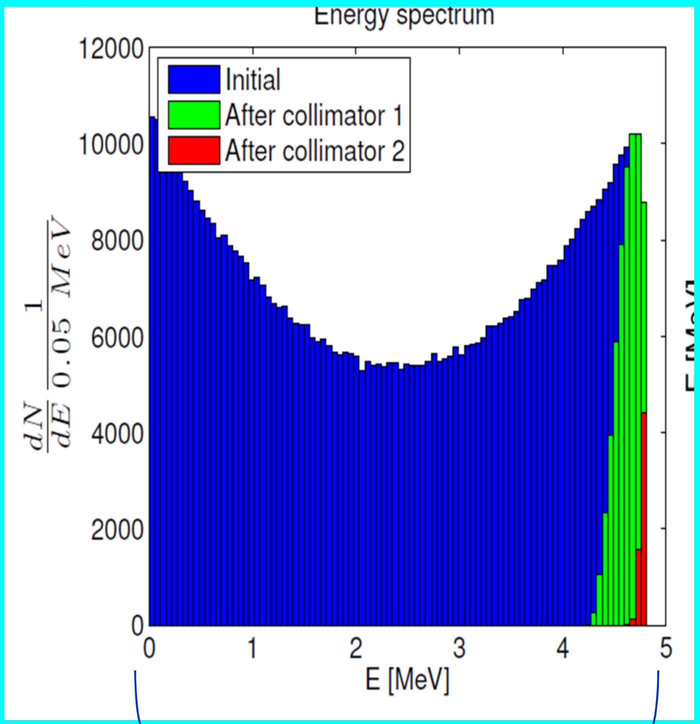

The most energetic photons are emitted on or close to the axis

By selecting the photons on axis with a system of collimators one can reduce conveniently the bandwidth.

White spectrum

I.Chaikovska and A. Variola

Angle-frequency correlation

$$\nu = \nu_L \frac{1 - \underline{e}_k \cdot \underline{\beta}_0}{1 - \underline{n} \cdot \underline{\beta}_0 + \frac{h\nu_L}{mc^2 \gamma_0}\left(1 - \underline{e}_k \cdot \underline{n}\right)}$$

Collecting the radiation in an acceptance angle θ>>1/γ, the spectrum is white.

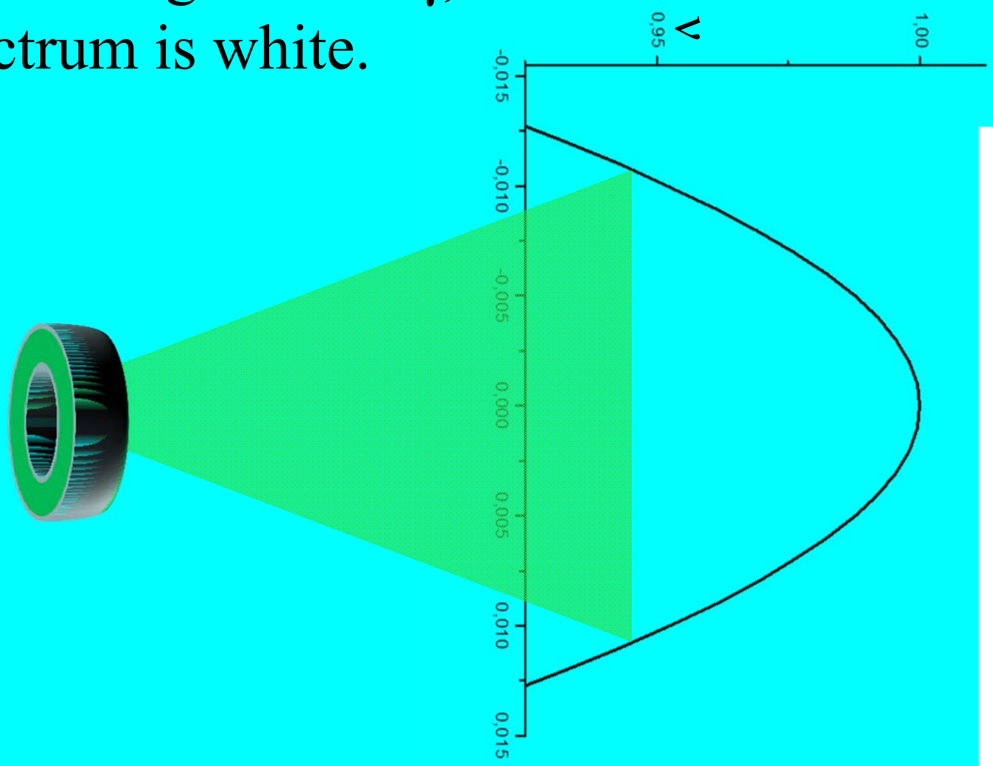

CAIN results

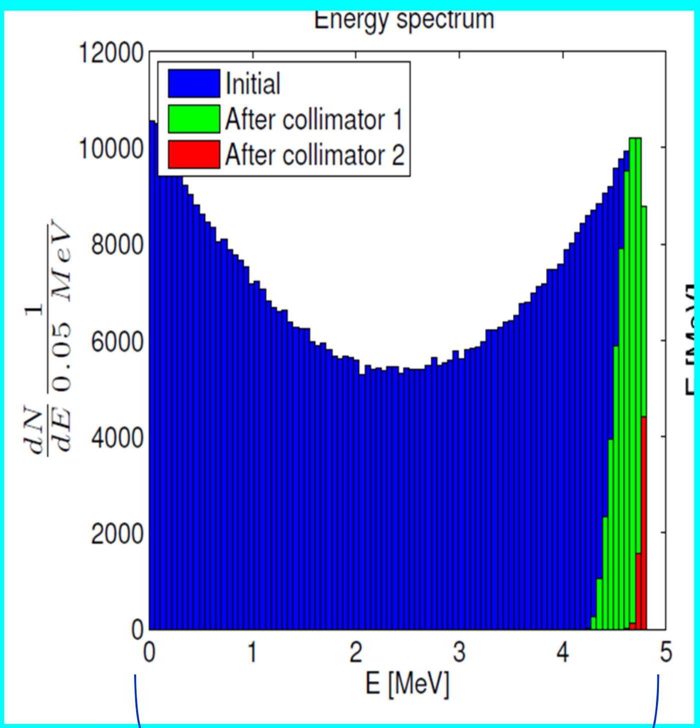

The most energetic photons are emitted on or close to the axis

By selecting the photons on axis with a system of collimators one can reduce conveniently the bandwidth.

White spectrum

I.Chaikovska and A. Variola

Angle-frequency correlation

$$\nu = \nu_L \frac{1-\underline{e}_k\cdot\underline{\beta}_0}{1-\underline{n}\cdot\underline{\beta}_0+\frac{h\nu_L}{mc^2\gamma_0}(1-\underline{e}_k\cdot\underline{n})}$$

Collecting the radiation in an acceptance angle θ>>1/γ, the spectrum is white.

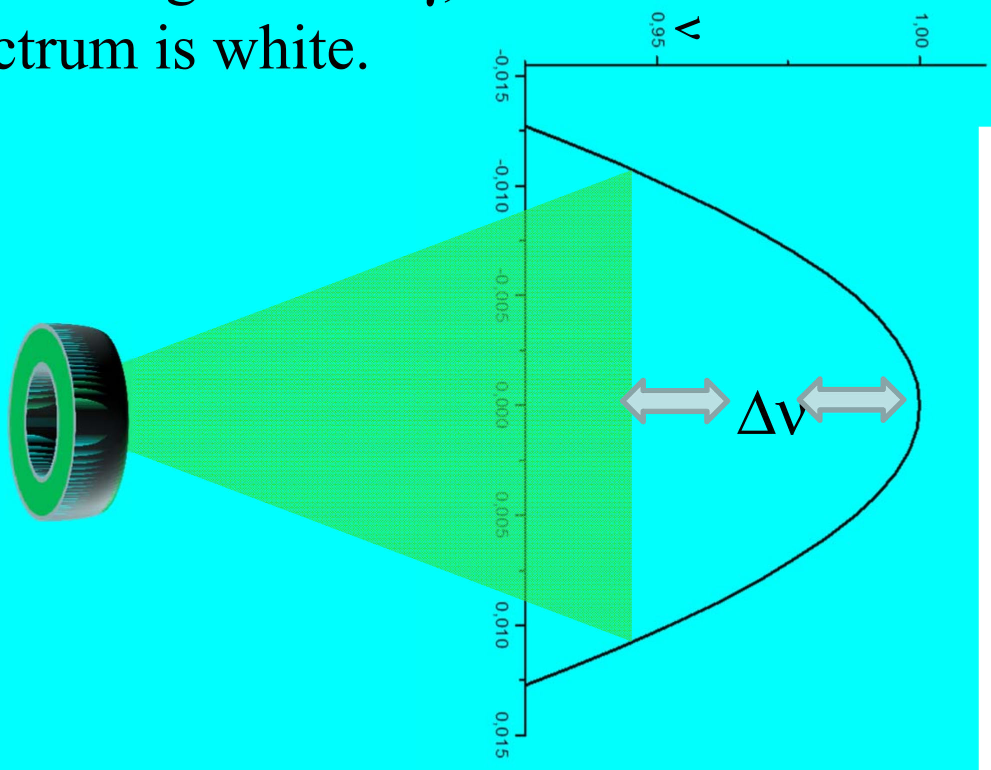

CAIN results

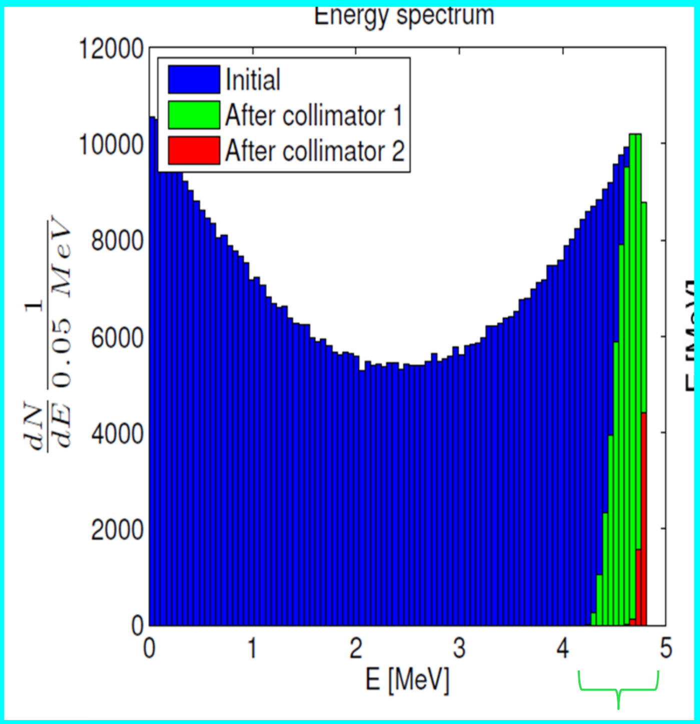

The most energetic photons are emitted on or close to the axis

Δν

By selecting the photons on axis with a system of collimators one can reduce conveniently the bandwidth.

White spectrum

I.Chaikovska and A. Variola

Angle-frequency correlation

$$\nu = \nu_L \frac{1 - \underline{e}_k \cdot \underline{\beta}_0}{1 - \underline{n} \cdot \underline{\beta}_0 + \frac{h\nu_L}{mc^2\gamma_0}\left(1 - \underline{e}_k \cdot \underline{n}\right)}$$

Collecting the radiation in an acceptance angle θ>>1/γ, the spectrum is white.

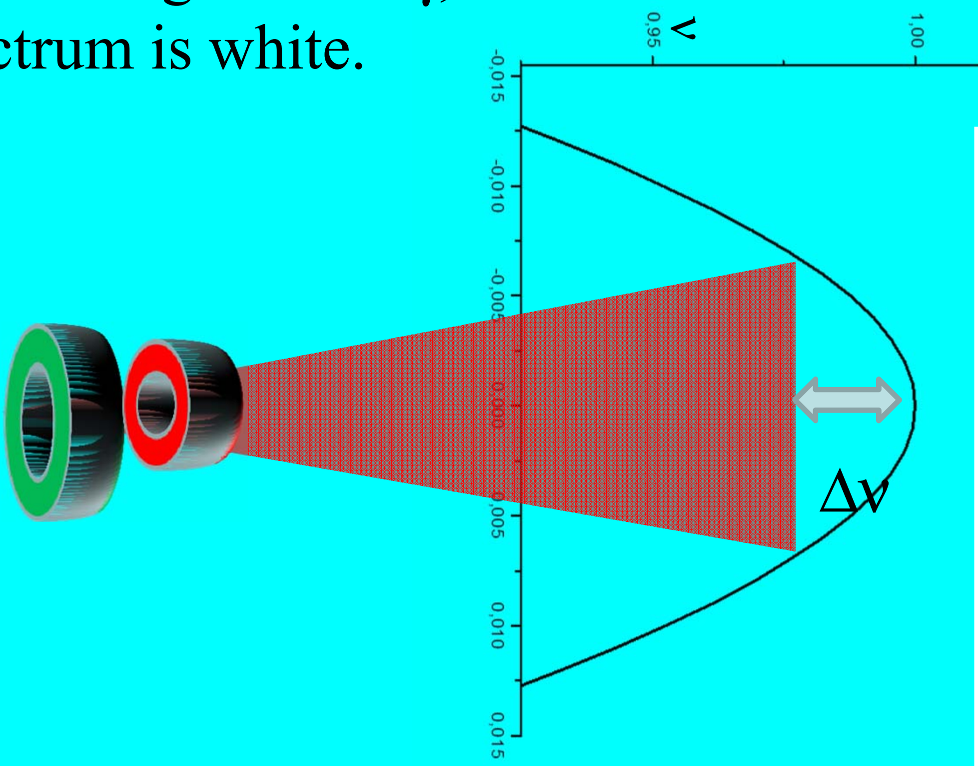

CAIN results

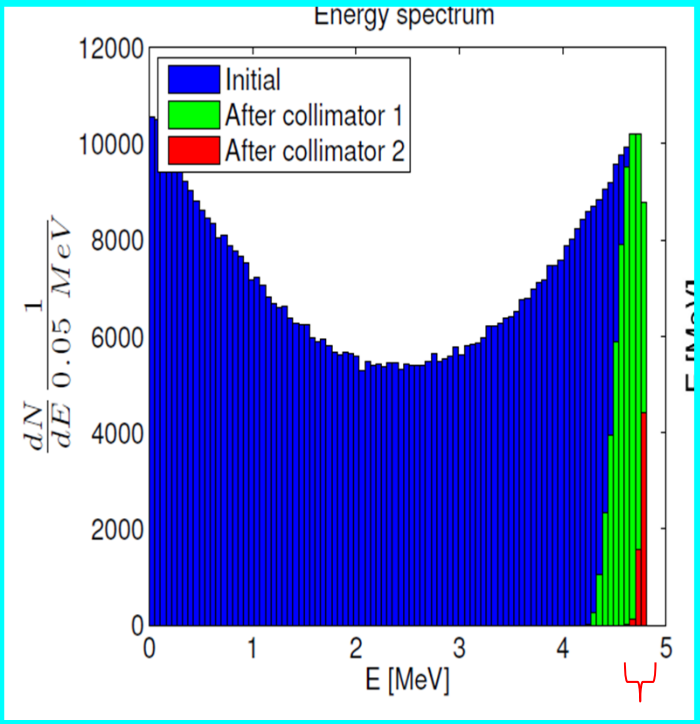

The most energetic photons are emitted on or close to the axis

Δν

By selecting the photons on axis with a system of collimators one can reduce conveniently the bandwidth.

White spectrum

I.Chaikovska and A. Variola

Quantum cross-section for electron-photon interaction (Klein and Nishina)

Dirac Equation: $$i\frac{\partial\psi}{\partial t} = (\hat{H}_0 + \hat{H}_{int})\psi$$

Radiation potential:

$$\hat{A} = hc\left(\underline{e}_L\sqrt{\frac{1}{\omega_L}}\left(e^{i(\underline{k}_L\cdot\underline{r}-\omega_L t)}\hat{a}_L + e^{-i(\underline{k}_L\cdot\underline{r}-\omega_L t)}\hat{a}_L{}^{+}\right) + \underline{e}\sqrt{\frac{1}{\omega}}\left(e^{i(\underline{k}\cdot\underline{r}-\omega t)}\hat{a} + e^{-i(\underline{k}\cdot\underline{r}-\omega t)}\hat{a}^{+}\right)\right)$$

Transition probability (perturbation theory or Feyman-Dyson graphs):

$$w_{n,m} = \frac{2\pi}{\hbar}\rho\left|\sum_{n'}\frac{H_{m,n'}H_{n',n}}{E_m - E_{n'}} + \sum_{n'}\frac{H_{m,n''}H_{n'',n}}{E_m - E_{n''}}\right|^2$$

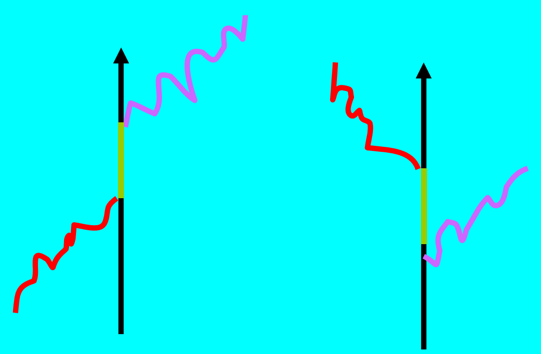

COMPARISON between classical (TSST), quantum semianalytical (Comp_cross) and quantum MonteCarlo (CAIN)

Number of photons

bandwidth

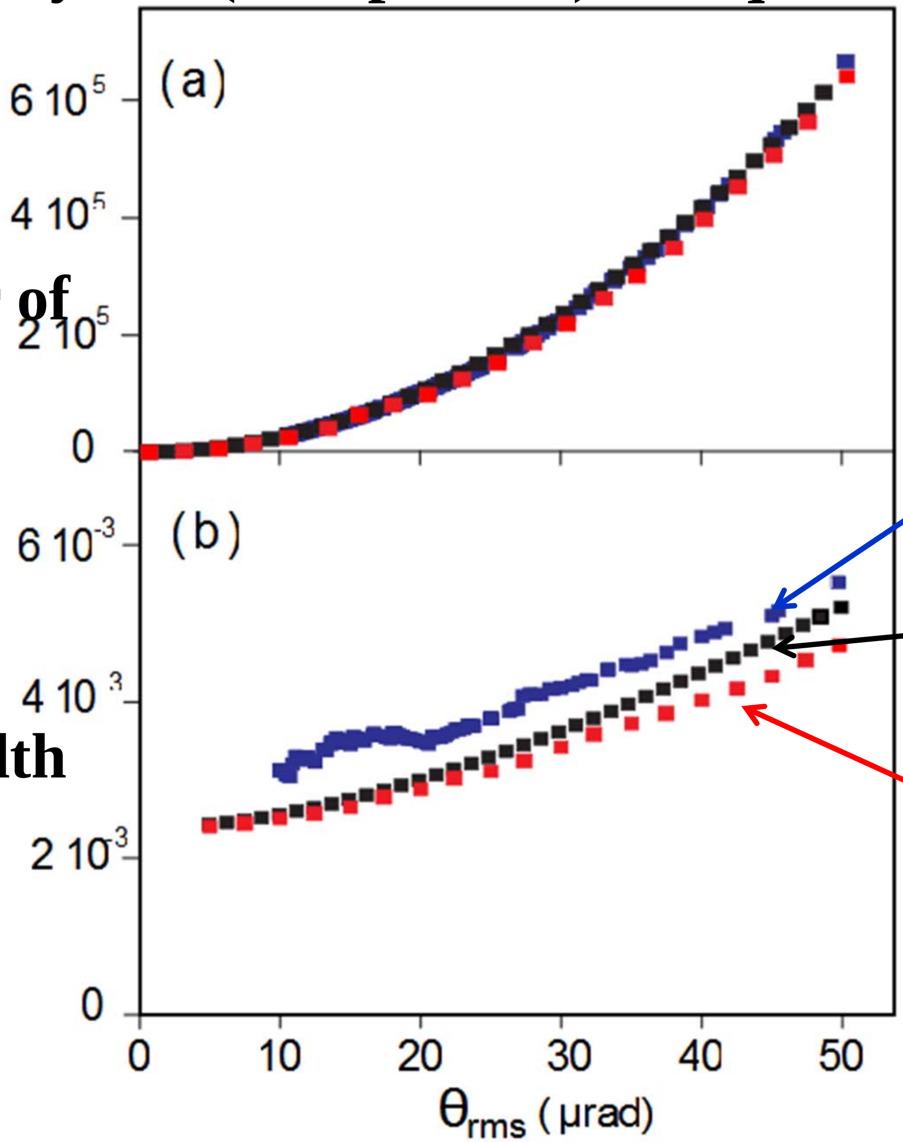

CAIN (quantum MonteCarlo)
Run by I.Chaichovska and A. Variola

TSST (classical)
Developed by P. Tomassini

Comp_Cross (quantum semianalytical)
Developed by V.Petrillo

Quantum shift ΔE

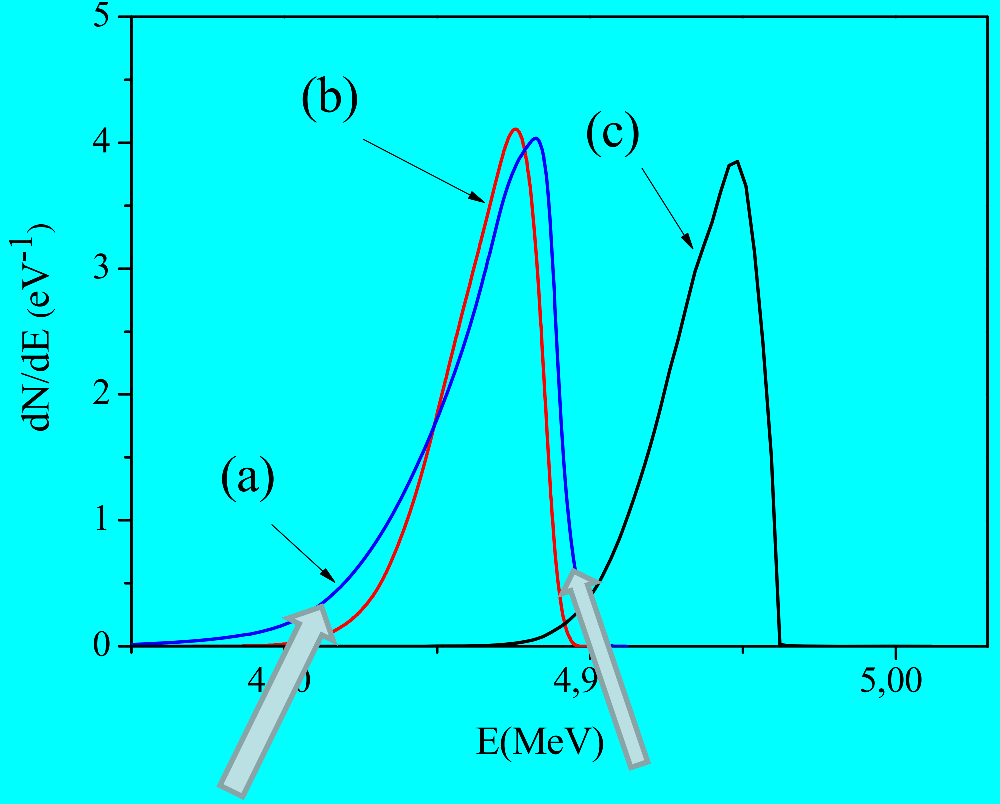

(a)CAIN
(b)Comp_Cross
(c)TSST

A part from the quantum shift, the spectra are very similar

Analytical Model based on Luminosity

Number of photons/shot within the rms bandwith

$$N = \frac{7.410^{9} E_L(J) Q(pC)\ \psi^2}{h\nu_L(eV)(w_0^2 + 2\sigma_x^2)\sqrt{1 + \frac{\delta^2(\sigma_x^2 + \sigma_{x,e}^2)}{(w_0^2 + 2\sigma_x^2)}}}$$

Bandwidth

$$\frac{\Delta\nu_\gamma}{\nu_\gamma} \cong \sqrt{\boxed{(\gamma\vartheta)^4} + \underbrace{4\left(\frac{\Delta\gamma}{\gamma}\right)^2 + \left(\frac{\varepsilon_n}{\sigma_x}\right)^4}_{\text{electron beam}} + \underbrace{\left(\frac{\Delta\nu}{\nu}\right)^2 + \left(\frac{M^2\lambda_L}{2\pi w_0}\right)^4 + \left(\frac{a_{0p}^2/3}{1+a_{0p}^2/2}\right)^2}_{\text{laser}}}$$

$\Psi = \gamma\vartheta$ *normalized rms collection angle*

$Optimized\ \ Bandwidth \cong (\varepsilon_n/\sigma_x)^2$

$Maximum\ \ Spectral\ \ Density \propto Luminosity/(\varepsilon_n/\sigma_x)^2 \propto Q/\varepsilon_n^2$

$Maximum\ \ Spectral\ \ Density \propto Phase\ \ Space\ \ density\ \ \eta_n$

Gamma-ray Source Specifications

$$Gamma-ray \quad Energy: \quad 1-20 \quad MeV$$

$$Bandwidth: \quad 0.3\% \rightarrow 0.1\%$$

$$Spectral \quad Density: \quad 10^4 \rightarrow 10^6 \quad photons/\mathrm{sec}/eV$$

$$rms \quad divergence \; < \; 200 \quad \mu rad$$

$$(spot \quad size \; < \; 5 \quad mm \quad at \quad \mathrm{target})$$

$$controllable > 98\% \quad polarization$$

1-2 orders of magn. better than state of the art

HiGS (bdw 3%, sp. dens. 10^2, E < 8 MeV)

Transverse Phase Space Density (round beams) : the chart (RF Photo-Injectors vs. Plasma Inj.)

$$\eta_n \equiv \frac{Q}{\varepsilon_n^2} \quad \left[\frac{pC}{(mm \cdot mrad)^2} \right]$$

0.1-1 psec bunches
RF

$$\eta_n \equiv \frac{Q}{\varepsilon_n^2}$$

fsec bunches
laser-plasma

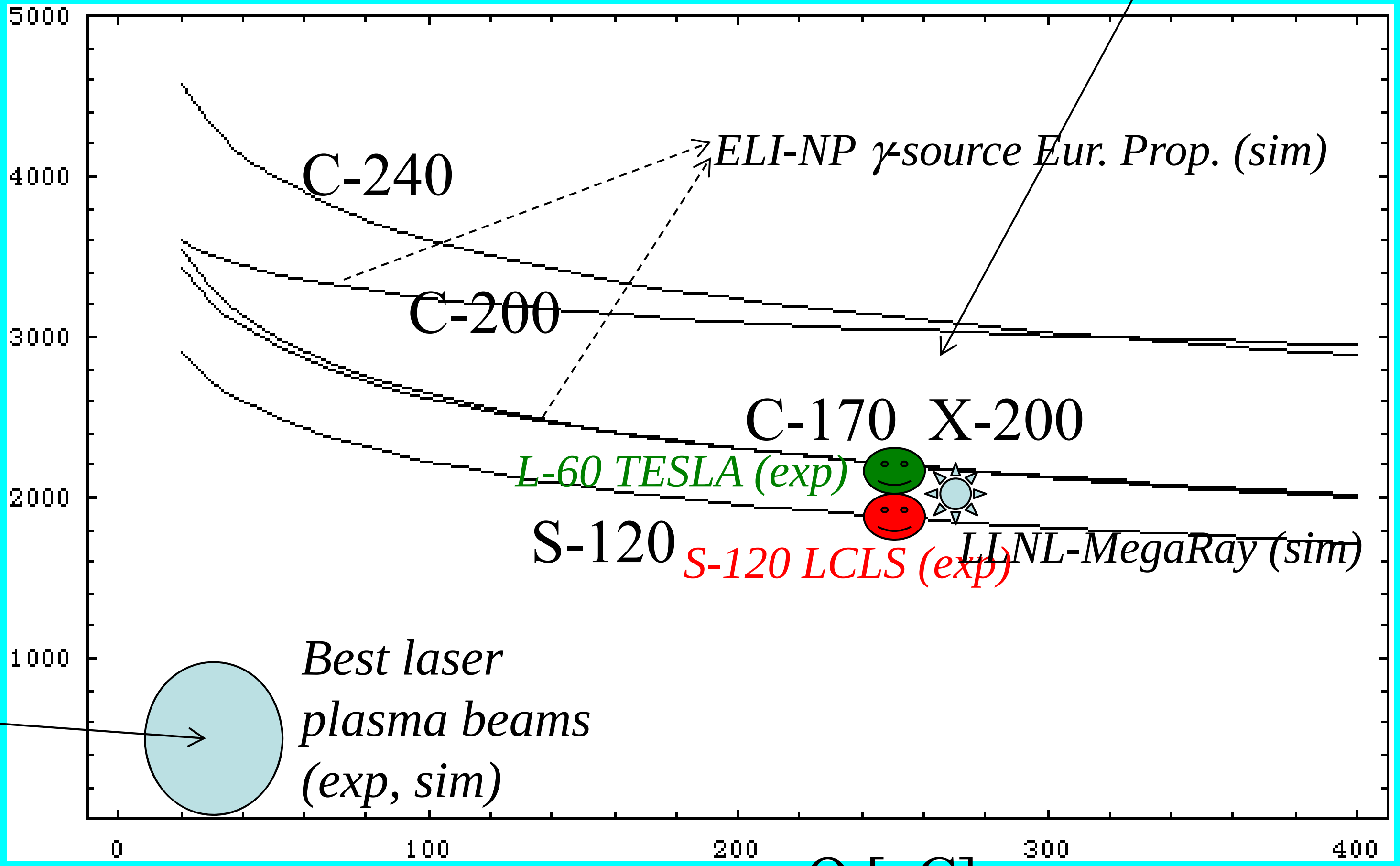

Q [pC]

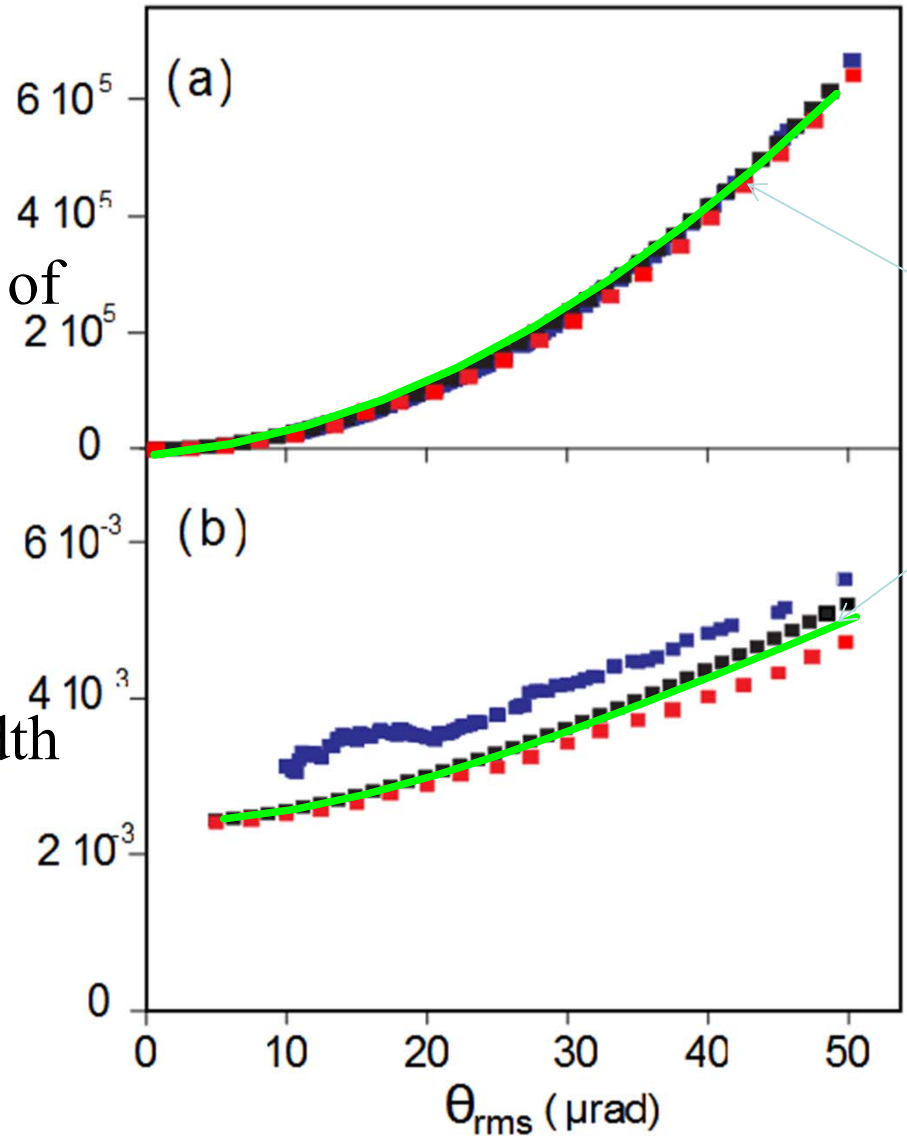

Number of photons

bandwidth

Scaling laws

Marrying Lasers and Particle Beams

In Vacuum Acceleration

The Far Future?
The Perfect Beam Marriage in Vacuum

VACUUM LASER ACCELERATION EXPERIMENT PERSPECTIVE AT BROOKHAVEN NATIONAL LAB-ACCELERATOR TEST FACILITY

X. Ding, L. Shao[#], D. Cline, UCLA, Los Angeles, CA 90095, USA
I. Pogorelsky, K. Kusche, M. Fedurin, V. Yakimenko, BNL, Upton, NY 11973, USA
Y.K. Ho, Q. Kong, Fudan University, Shanghai 200433, China
J. J. Xu, Shanghai Institute of Optics and Fine Mechanics, Shanghai 201800, China

WEPPP008

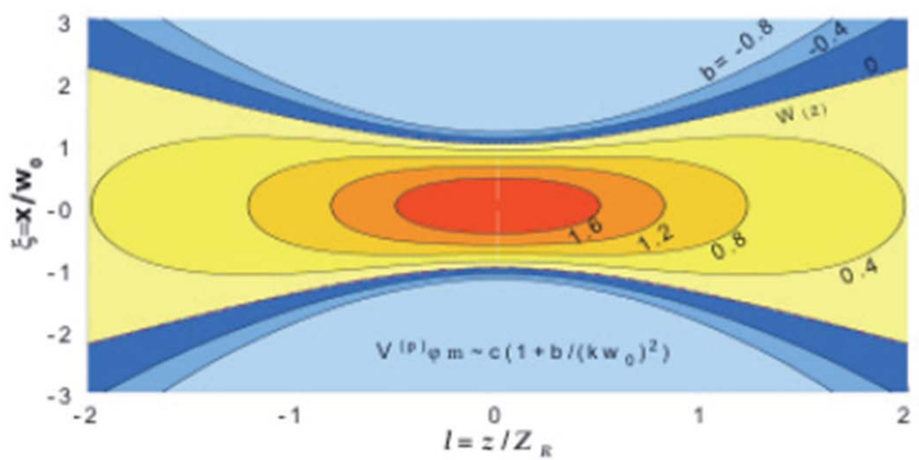

Figure 1: The distribution of the minimum phase velocity v_* in the plane y=0.

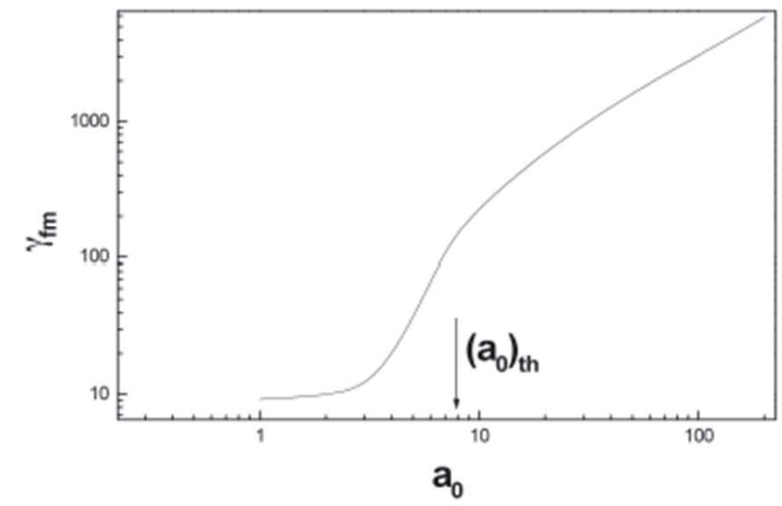

Figure 3: Final energy as a function of laser intensity a_0.

Challenge for Phase Space Density
of Injected Beam at low energy (time jitter)

ACKNOWLEDGMENTS

I am indebted to Vittoria Petrillo, Luca Giannessi, Pietro Musumeci and Xiaoping Ding for providing material for this presentation and for many helpful discussions

Angular and Frequency Spectrum
(560 MeV electrons)

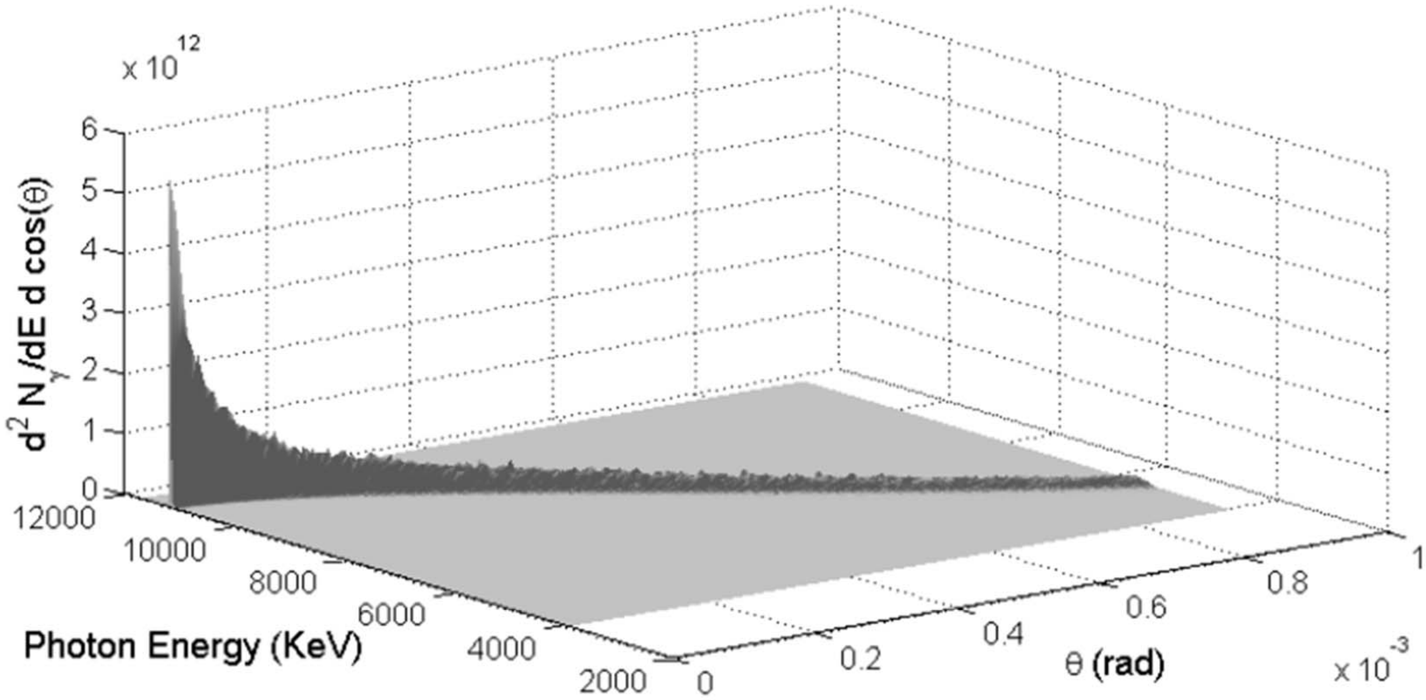

Figure 18: Spectrum versus photon energy and collection angle

Scattered photons in collision

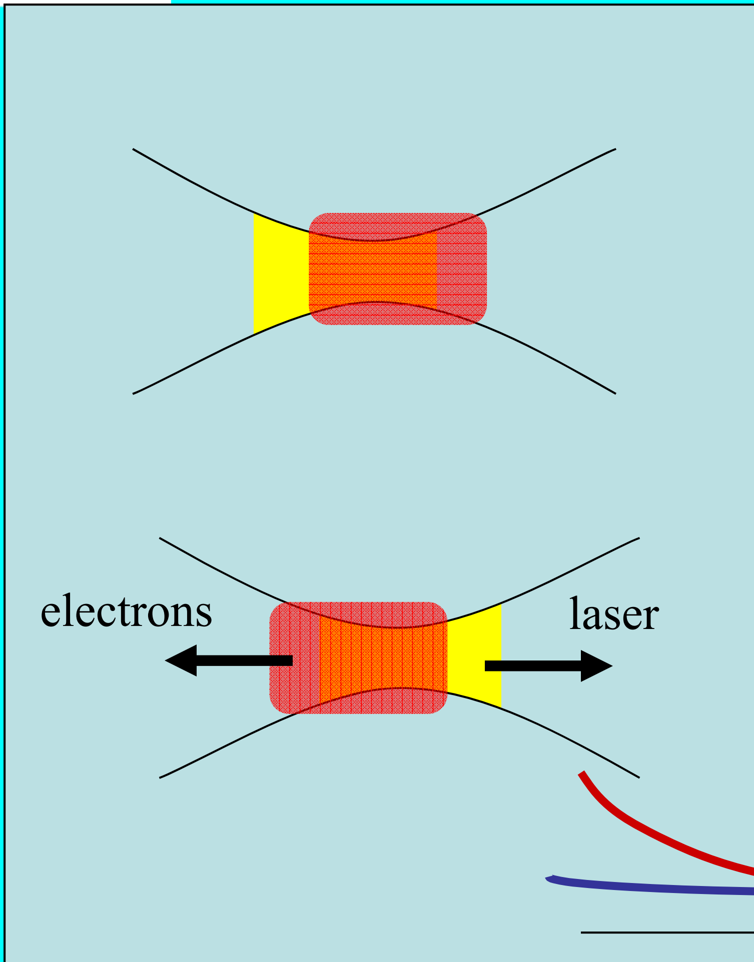

Thomson cross-section

$\sigma_T = 0.67 \cdot 10^{-24} \, cm^2 = 0.67 \;\; barn$

- Scattered flux $\boxed{N_\gamma = \mathbf{L}\sigma_T}$ $\boxed{\sigma_T = \frac{8\pi}{3} r_e^2}$
- Luminosity as in HEP collisions
  - Many photons, electrons
  - Focus tightly $\boxed{\mathbf{L} = \frac{N_L N_{e-}}{4\pi\sigma_x^2}}$

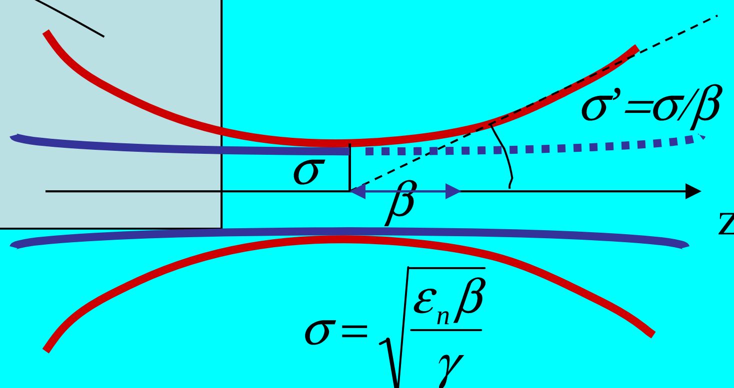

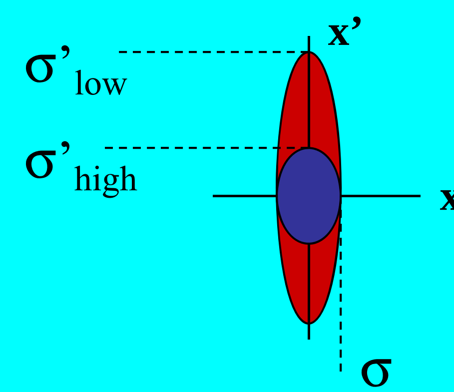

Spectral broadening due to ultra-focused beams:
Thomson Source classically described as a
Laser Syncrotron Light Source

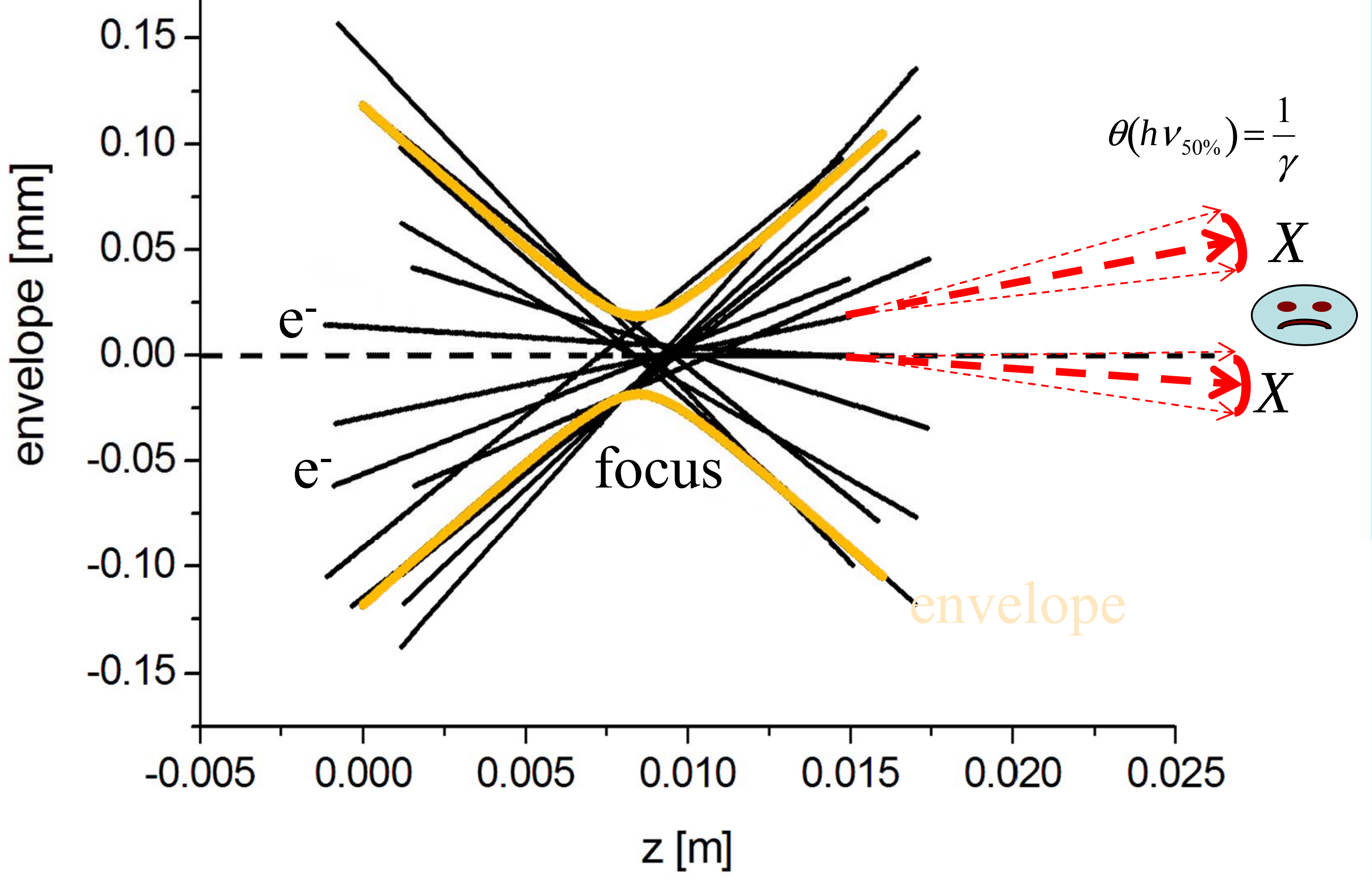

Scattering angle in Thomson limit (no recoil) is small, i.e. < $1/\gamma$

Spectral broadening due to ultra-focused beams:
Thomson Source classically described as a
Laser Syncrotron Light Source

$$\theta(h\nu_{50\%}) = \frac{1}{\gamma}$$

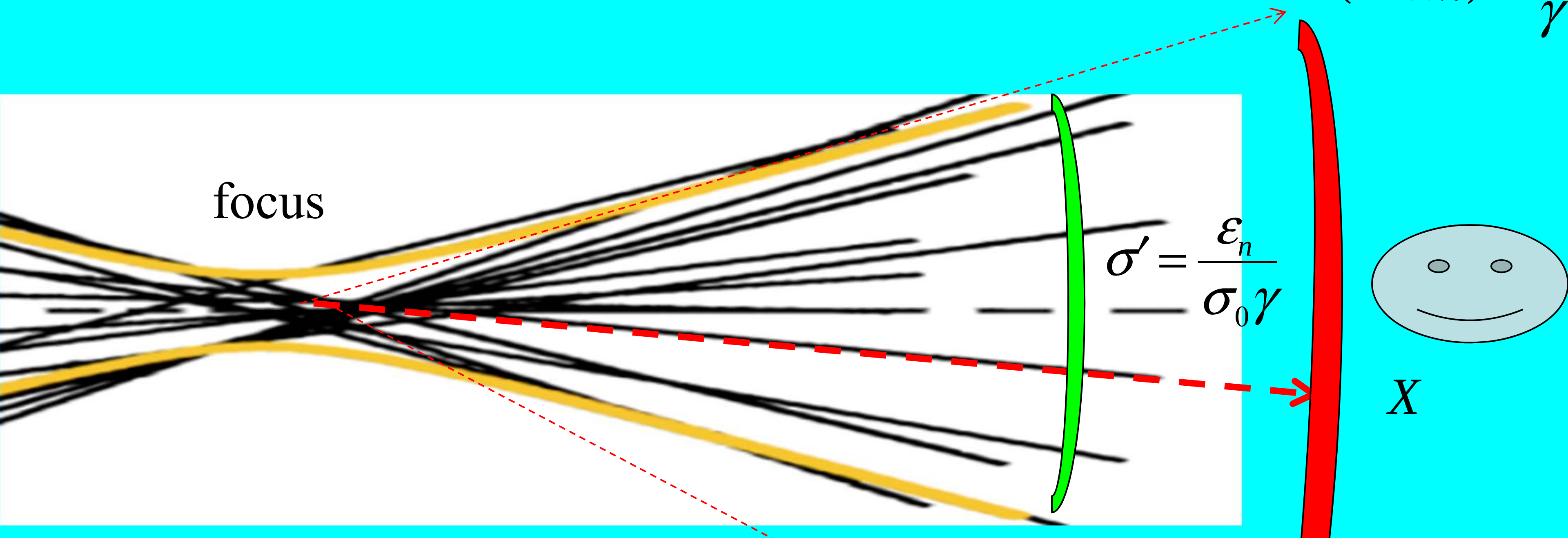

$$\sigma' = \frac{\varepsilon_n}{\sigma_0 \gamma} << \frac{1}{\gamma} \quad \Rightarrow \quad \frac{\varepsilon_n}{\sigma_0} << 1 \quad \Rightarrow \quad \sigma_0 >> \varepsilon_n$$

Limit to focusability due to max acceptable bandwidth

T=2.5ps vs T=10ps, α=0deg

- A ponderomotive redshift is clearly visible. Ψ=1e-2

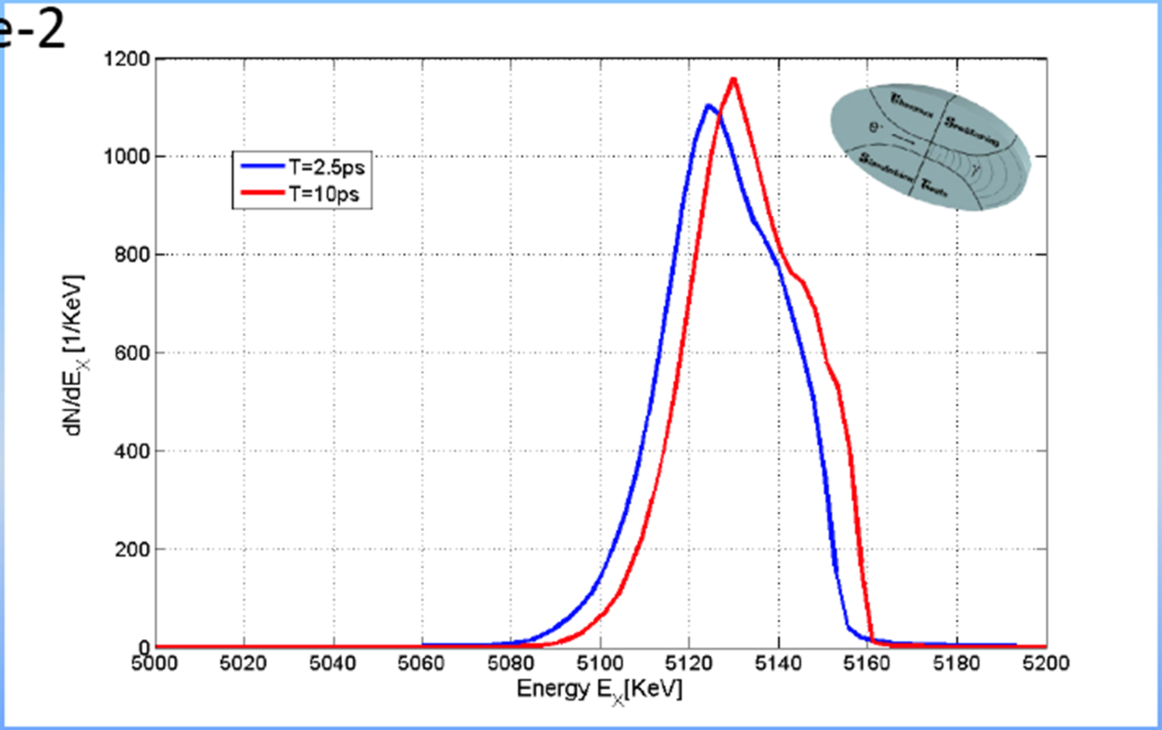

Courtesy P. Tomassini

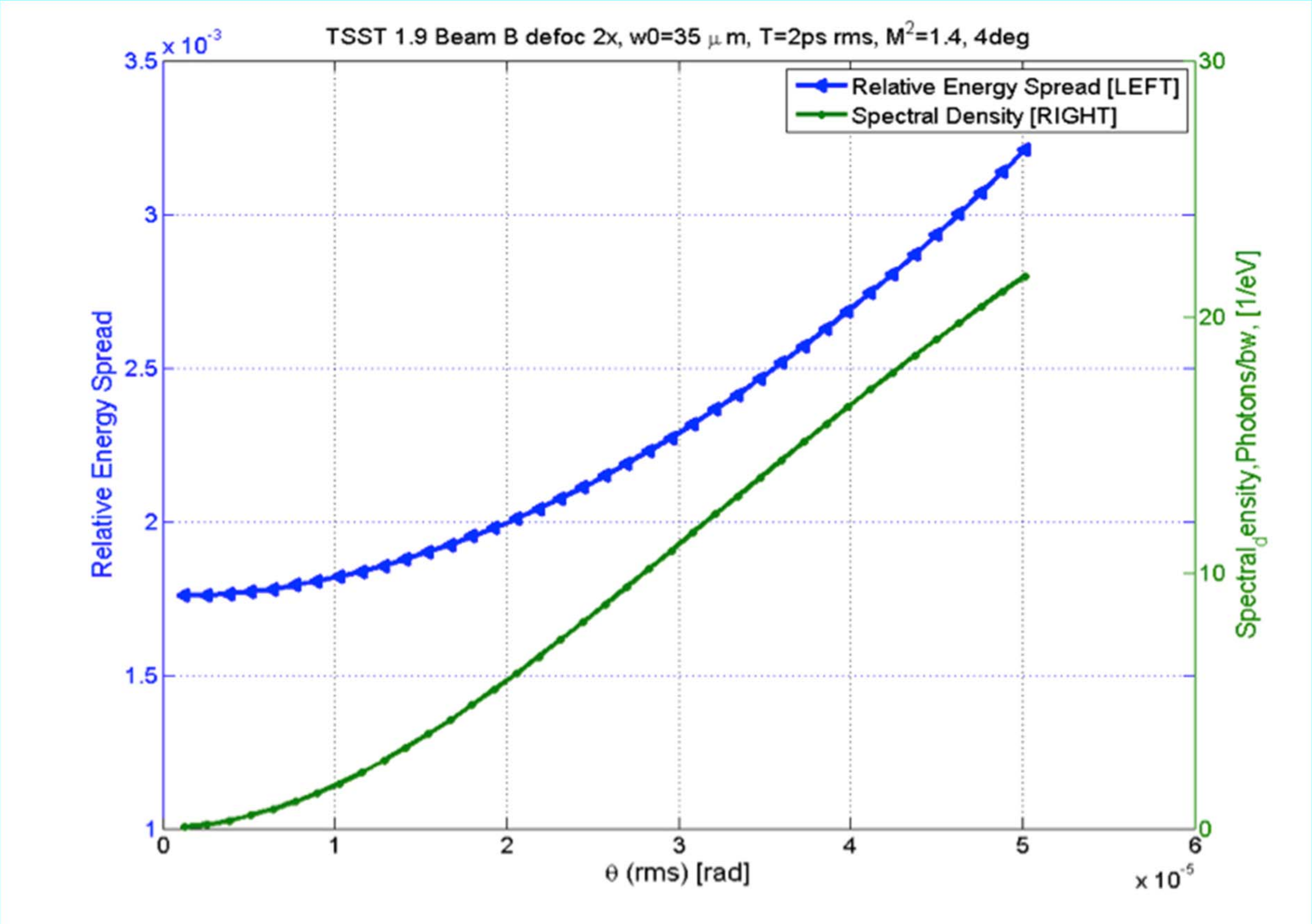

TSST 1.9 Beam B defoc 2x, w0=35 μm, T=2ps rms, M²=1.4, 4deg
Relative Energy Spread [LEFT]
Spectral Density [RIGHT]
Relative Energy Spread
Spectral_density,Photons/bw, [1/eV]
θ (rms) [rad]
x 10^-3
x 10^-5
3.5
3
2.5
2
1.5
1
0
1
2
3
4
5
6
30
20
10
0

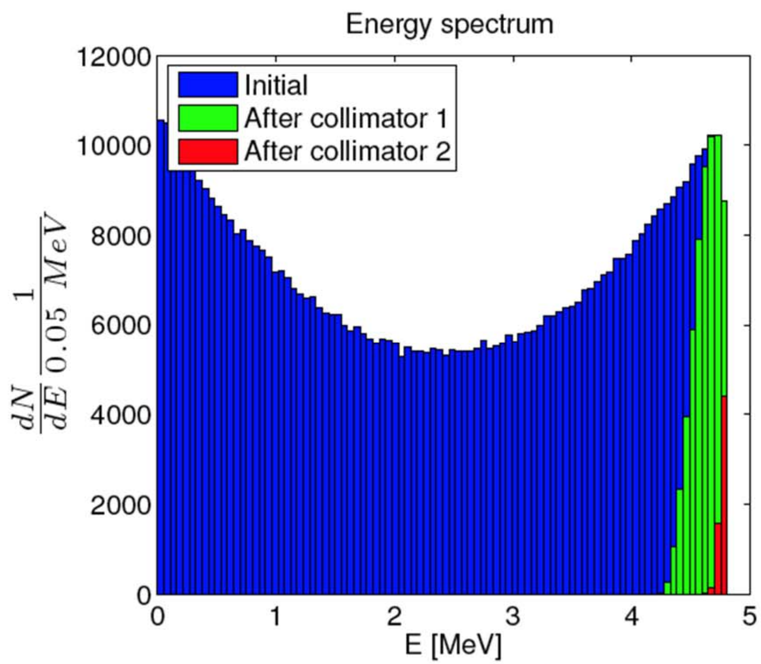

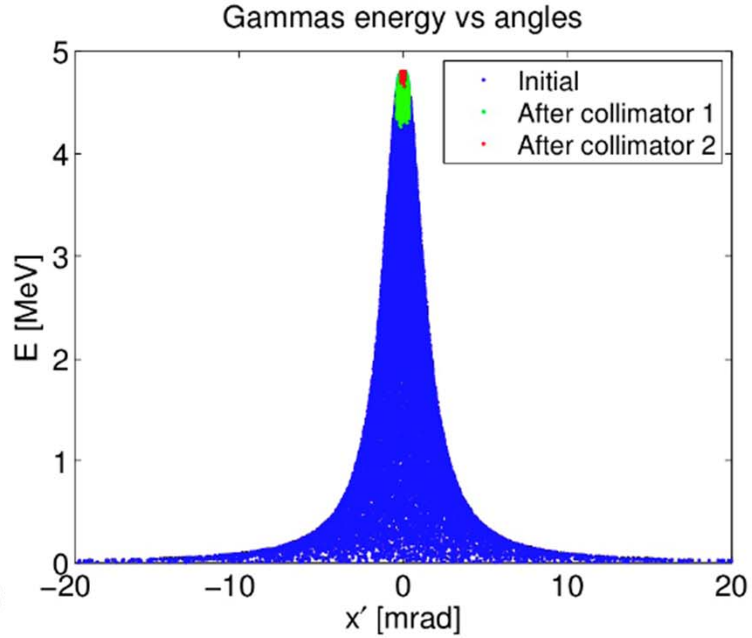

Photon extraction line

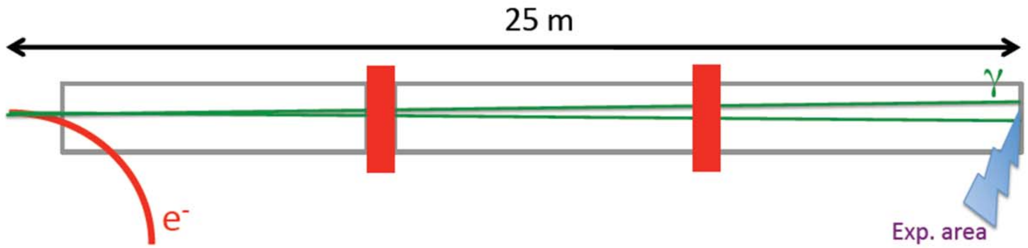

- Collimator 1 : d=11 m r= 0.3 cm , t= 5 cm (W)
- Collimator 2 : d=15 m r= 0.1 cm, t= 5 cm (W)
- Beam pipe r=2cm t=0.1 cm (Fe)
- Emax < 10 MeV : below giant resonance
  Geant4 hadronic processes switch off

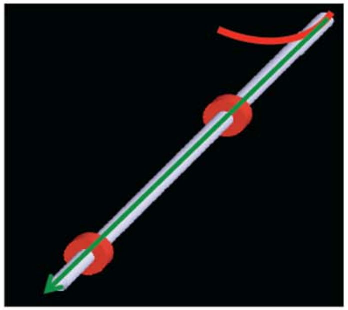

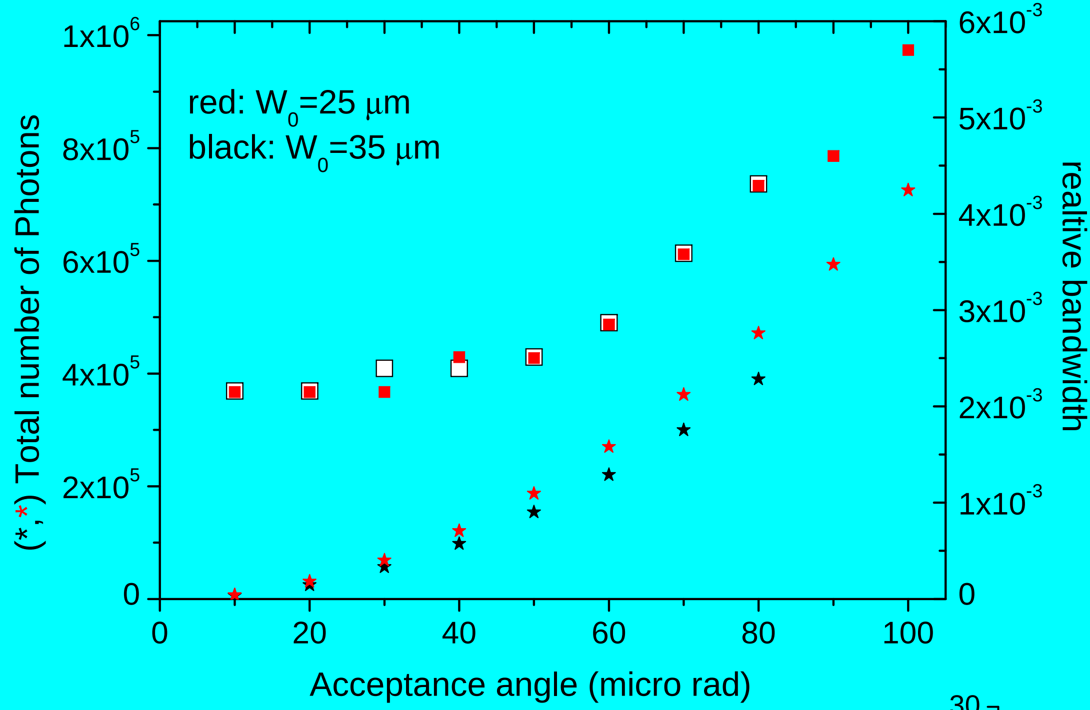

Total Number and bandwidth vs. acceptance angle

Photon number per eV vs. acceptance angle

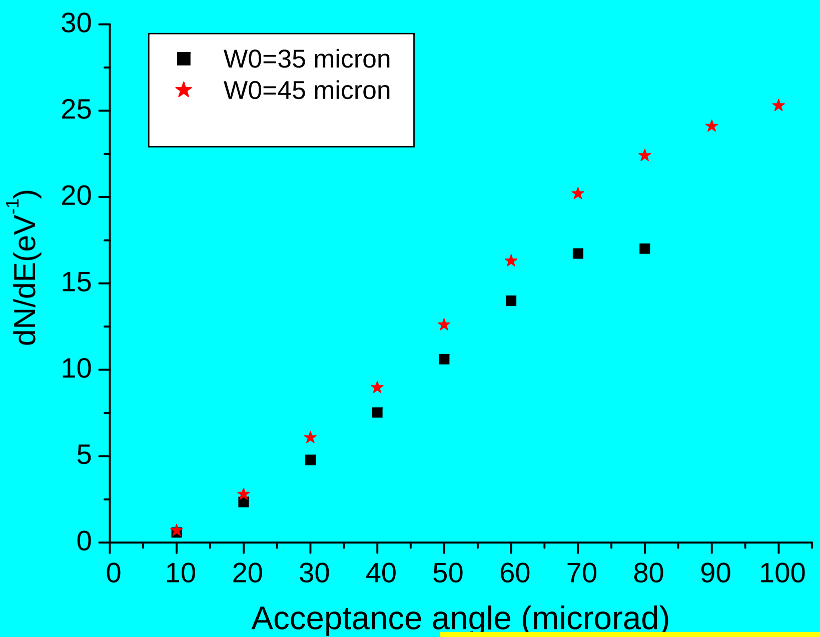

Courtesy V. Petrillo

FEL resonance condition

$$\lambda_R = \lambda_w \frac{\left(1 + a_w{}^2\right)}{2\gamma^2}$$

(magnetostatic undulator)

Example : for λ_R=*1A*, λ_w=*2cm, E=7 GeV*

$$a_w = 0.93\lambda_w[cm]B_w[T]$$

$$\lambda_R = \lambda \frac{\left(1 + a_0^2/2\right)}{4\gamma^2}$$

(electromagnetic undulator)

Example : for λ_R=*1A*, λ=*0.8*μ*m, E=25MeV*

$$a_0 = 4.8\frac{\lambda[\mu m]\sqrt{P[TW]}}{R_0[\mu m]}$$

laser power

laser spot size